

# Class-aware and Augmentation-free Contrastive Learning from Label Proportion

Jialiang Wang<sup>1</sup>, Ning Zhang<sup>3</sup>, Shimin Di<sup>1</sup>, Ruidong Wang<sup>4</sup>, Lei Chen<sup>2,1</sup>

<sup>1</sup>The Hong Kong University of Science and Technology, Hong Kong SAR, China

<sup>2</sup>The Hong Kong University of Science and Technology (Guangzhou), Guangzhou, China

<sup>3</sup>Tencent America, Palo Alto, CA, USA

<sup>4</sup>Tencent Europe B.V., Amsterdam, North Holland, Netherlands

{jwangic, sdiaa}@connect.ust.hk, {drningzhang, ruidwang}@global.tencent.com, leichen@cse.ust.hk

## ABSTRACT

Learning from Label Proportion (LLP) is a weakly supervised learning scenario in which training data is organized into predefined bags of instances, disclosing only the class label proportions per bag. This paradigm is essential for user modeling and personalization, where user privacy is paramount, offering insights into user preferences without revealing individual data. LLP faces a unique difficulty: the misalignment between bag-level supervision and the objective of instance-level prediction, primarily due to the inherent ambiguity in label proportion matching. Previous studies have demonstrated deep representation learning can generate auxiliary signals to promote the supervision level in the image domain. However, applying these techniques to tabular data presents significant challenges: 1) they rely heavily on label-invariant augmentation to establish multi-view, which is not feasible with the heterogeneous nature of tabular datasets, and 2) tabular datasets often lack sufficient semantics for perfect class distinction, making them prone to suboptimality caused by the inherent ambiguity of label proportion matching. To address these challenges, we propose an augmentation-free contrastive framework TabLLP-BDC that introduces class-aware supervision (explicitly aware of class differences) at the instance level. Our solution features a two-stage Bag Difference Contrastive (BDC) learning mechanism that establishes robust class-aware instance-level supervision by disassembling the nuance between bag label proportions, without relying on augmentations. Concurrently, our model presents a pioneering multi-task pretraining pipeline tailored for tabular-based LLP, capturing intrinsic tabular feature correlations in alignment with label proportion distribution. Extensive experiments demonstrate that TabLLP-BDC achieves state-of-the-art performance for LLP in the tabular domain.

## KEYWORDS

Learning from label proportion, weakly supervised learning, contrastive learning, privacy-preserving data handling

## 1 INTRODUCTION

Learning from Label Proportions (LLP) is a weakly supervised learning paradigm organizing training data into predefined bags of instances, where only the proportion of each class within these bags is known. Its primary goal is to develop an instance-level classifier capable of predicting labels for individual instances, overcoming the constraints of aggregated labels [36, 43]. This capability is crucial for tailoring personalized web experiences, enabling the derivation of meaningful insights for privacy-preserving content delivery

and advertising strategies [4, 67] from bag-level proportional labels shared in business collaborations [38]. Extensively applied in online advertising, examples include platforms like Google Ads [12] and Facebook Ad Platform [11], alongside privacy-preserving strategies such as aggregated reporting and K-anonymity principles [52]. LLP strikes a balance between enhancing user experience and maintaining privacy by leveraging aggregated data to reduce risks associated with detailed user profiles. Additionally, the cost-efficiency of storing aggregated data is particularly beneficial for large databases [2]. LLP offers a practical solution in scenarios where storing detailed user data is unnecessary, such as electoral campaigns [42, 51] or demographic categorization [1], allowing businesses to economically derive instance-level insights from aggregated data storage.

Advancing LLP methodologies necessitates addressing the inherent difficulty of aligning bag-level training objectives with instance-level predictions. Research in LLP has predominantly focused on the label proportion matching principles to train classifiers that accurately reflect observed label proportions [71]. Traditional LLP models, such as SVMs [17, 42], Bayesian models [22], and clustering techniques [49], were mainly designed for binary classification and faced scalability issues. The advent of deep representation learning introduced a significant shift, leveraging deep neural models for extensive, multi-dimensional LLP predictions in the image domain [1, 33, 34, 55]. These models often utilize bag-level Cross-entropy [15] loss to facilitate end-to-end learning in multiclass settings. However, a closer examination reveals a critical, yet often overlooked, difficulty in LLP: the misalignment between bag-level training objectives and instance-level predictions. This difficulty stems from the inherent ambiguity in label proportion matching, where multiple instance-level label distributions could feasibly correspond to identical bag-level label proportions [30]. Although barely formally defined or theoretically analyzed, successful image-based LLP methods have employed instance-level supervision to address this challenge, as summarized in Tab. 1. These deep LLP models, tailored for image data, utilize methods such as adversarial autoencoders [62], Self-supervised learning [32], and prototypical contrastive clustering [30], capitalizing on label-invariant augmentations like image rotation [32] to achieve effective instance-level supervision without individual labels. Notably, contrastive-based models [30] have demonstrated particular promise by generating instance-level contrastive signals between multiple views from single instances.

The urgency for applying LLP to tabular data has intensified, especially in sectors like e-commerce and online advertising, where balancing privacy with personalized analysis became crucial [38].

**Table 1: Comparison of existing works in Deep LLP.**

Deep LLP Strategy	Scenario	Pretraining	Augmentation	Fine-tuning		
	Data Type	Task	Technique	Principle	Ins. Sup.	Class-aware
DLLP [1]	Image/Text	pre-trained weights	-	Batch Averager	×	-
ROT [15]	Image	pre-trained weights	label-invariant	Relax-OT Loss	✓	✓
LLP-VAT [55]	Image	pre-trained weights	VAT	Consistency Regularization	✓	×
LLP-PLOT [34]	Image	pre-trained weights	mixup	OT-based Pseudo-labeling	✓	✓
SELF-LLP [32]	Image	Self-supervised	label-invariant	Self-supervised & -ensemble	✓	✓
LLP-GAN [33]	Image/Text	-	label-invariant	GAN	✓	×
LLP-AAE [62]	Image	-	label-invariant	Adversarial Autoencoder	✓	×
LLP-Co [30]	Image	pre-trained weights	label-invariant	Prototypical Contrastive	✓	✓
SelfCLR-LLP [37]	Tabular	-	free	Self-contrastive	✓	×
TabLLP-BDC (Ours)	Tabular	Bag Contrastive	free	Bag Difference Contrastive	✓	✓

**Notations:** **pre-trained weights** indicate either the model explicitly uses a pretrained model on ImageNet [10] or adopts a backbone model for which a publicly available pretrained version exists. **label-invariant** means adopting label-invariant augmentations, such as image rotation, while **free** refers to an augmentation-free method. **Ins. Sup.** indicates the proposed method introduces instance-level supervision, and **Class-aware** means the instance-level supervision is explicitly aware of class differences.

While native contrastive learning [30] has proven effective in image-based LLP, it encounters significant challenges with tabular data. First, the heterogeneous and sensitive nature of tabular datasets compromises the feasibility of label-invariant augmentation techniques [20], which are essential for generating effective positive and negative pairs or multi-view in native contrastive learning. This is because tabular data can be extremely fragile to tiny perturbations [5], especially when manipulating categorical features, thus highlighting the necessity for an augmentation-free contrastive approach. Moreover, the inherent inconsistency and absence of spatial interdependencies and semantics within tabular data diminish the robustness essential for perfect class distinction [20]. Such limitations exacerbate the suboptimality of relying exclusively on matching label proportions and auxiliary losses that lack explicit class distinction, or *class-awareness*, at the instance level, intensifying the inherent difficulty of LLP. Consequently, there is a pronounced need for an augmentation-free and *class-aware* contrastive-based LLP approach, which should be meticulously designed to accommodate the specific characteristics of tabular data.

Recently, SelfCLR-LLP [37] has pioneering work in tabular-based deep LLP, utilizing Self-contrastive auxiliary loss as an instance-level signal to foster diversity in representation without augmentation. However, as summarized in Tab. 1, this approach falls short of relying predominantly on a classical Self-supervised formulation without any incorporation of label proportions, thus failing to offer the crucial *class-aware* guidance necessary for precise class distinction at the instance level. This limitation underscores a significant gap in achieving a tailored and effective contrastive solution for tabular-based LLP that can effectively utilize ambiguous label proportions for *class-aware* instance-level supervision without the need for augmentation. Beyond this, no existing work proposes a pretraining pipeline tailored for tabular-based LLP, despite the promising prospects of LLP as a weakly supervised learning framework for pretraining endeavors.

To address these challenges, we present TabLLP-BDC, a two-stage Bag Difference Contrastive (BDC) framework crafted to effectively navigate the intricacies of tabular-based LLP through *class-aware* and augmentation-free contrastive learning. Our Difference

Contrastive fine-tuning technique harnesses label proportion differences between bags to establish augmentation-free instance-level supervision that is explicitly aware of class distinctions—facilitating similar representations for instances within the same class and divergent representations across classes, a notable challenge in the absence of explicit instance-level labels. Additionally, TabLLP-BDC introduces a pioneering augmentation-free and multi-task Bag Contrastive pretraining pipeline tailored for tabular-based LLP, capturing intrinsic tabular feature correlations in alignment with label proportion distribution. Our main contributions include:

- We delve into the realm of LLP within tabular data domains, identifying and addressing unique challenges that hinder the development of current deep LLP methodologies due to the inherent properties of tabular datasets.
- We introduce a novel bag contrastive learning framework tailored for tabular-based LLP that circumvents the need for label-invariant augmentations. By leveraging a Linear Sum Assignment Problem [9] to generate pseudo-positive pairs between bags with proportional labels, our approach facilitates *class-aware* instance-level supervision without relying on explicit instance-level labels.
- We pioneer a multi-task pretraining phase specially designed for the tabular-based LLP to capture intrinsic tabular feature correlations that resonate with label proportion distribution. Incorporating a novel Bag Contrastive task in the metric learning manner at the bag level, our approach further refines the efficacy of native Self-contrastive pretraining pipeline [47] and ensures a seamless transition to downstream LLP training.
- We conducted thorough experiments on various public and real-world tabular datasets using different bagging strategies and bag sizes. Our analysis included both traditional LLP with instance-level validation and practical LLP with bag-level validation, introducing a novel evaluation metric, mPIoU, for the latter. Our TabLLP-BDC consistently delivers SOTA instance-level performance. Additionally, we conducted extensive ablation studies to assess each model component’s impact and effectiveness.

## 2 RELATED WORK

### 2.1 Learning from Label Proportion

Weakly Supervised learning (WSL) [25, 74] emerges as a pragmatic alternative to fully supervised learning, especially in domains where obtaining dense and accurate labels is expensive or infeasible [42]. In its essence, WSL utilizes weak labels, which can be incomplete [41, 45, 53], inaccurate [14, 72, 73], or inexact [50, 54, 61], to train machine learning models effectively [74]. Among them, tasks using inexact labels without precise instance-level details have gained attention recently. A prominent example of such a task is Multiple Instance Learning (MIL) [23, 50, 54, 61], where models are trained on group-level labels and also make predictions at the group level.

However, there exists a particularly intriguing and less explored paradigm called Learning from Label Proportion (LLP). In the LLP framework, data is provided as bags of instances. A bag denoted as  $B_k$ , comprising  $m$  instances. Each bag is associated with a label proportion vector  $\bar{\mathbf{p}}_k$ , where each entry  $\bar{p}_k^c = \frac{1}{m} \sum_{i=1}^m y_{ki}^c$  specifies the proportion of instances from a particular class  $c$ , assuming  $\mathbf{y}_{ki}$  to be the potential one-hot label vector for instance  $x_{ki}$  within the bag  $k$ . The LLP dataset can then be defined as  $D_{LLP} = \{(B_k, \bar{\mathbf{p}}_k)\}_{k=1}^K$  with  $K$  being the total number of bags.

The uniqueness of LLP lies in its objective: while it is trained using group-level label proportions similar to MIL, it aims to make predictions at the instance level. Formally, the LLP problem is to learn an instance-level classifier  $f_\theta(\cdot)$  parameterized by  $\theta$  by minimizing an LLP loss function  $\mathcal{L}_{LLP}(\cdot, \cdot)$ , which aims to minimize the discrepancy between the predicted and actual label proportions  $\bar{\mathbf{p}}_k$ :

$$\theta^* = \arg \min_{\theta} \sum_{k=1}^K \mathcal{L}_{LLP} \left( \frac{1}{m} \sum_{i=1}^m f_\theta(x_{ki}), \bar{\mathbf{p}}_k \right) \quad (1)$$

where  $\mathcal{L}_{LLP}(\cdot, \cdot)$  generally denotes a suitable discrepancy measurement. This formulation introduces the preliminary approach to LLP: ensuring that the aggregated instance-level predictions within a bag closely match the given bag label proportion. More advanced approaches necessitate the model to discern intricate patterns both within and across bags to infer likely labels for individual instances.

**2.1.1 Traditional LLP.** The study of LLP in traditional machine learning began by reconfiguring supervised algorithms such as SVM, kNN, and Neural Network for aggregated outputs [36], with typical adaptations including reassigning instance labels with bag label proportions. In the probabilistic realm, hierarchical Bayesian models trained with MCMC samplers [29] or Structural EM [22] were introduced to address uncertainty. Other strategies included Mean Map models [43] that focus on mean operators for LLP optimization and clustering methods [7, 49] that emphasize the intricate relationship between data structures and label proportions. The SVM landscape was later expanded with pseudo-labels [17] and inverted conditional class probabilities estimation [44]. This era concluded with the EPRM framework [66] that aimed to minimize empirical bag proportion loss. Despite these advancements, traditional LLP methods faced issues with scalability, rigid assumptions, and limited efficacy in multi-class contexts.

**2.1.2 Deep LLP.** With the rise of deep learning, LLP witnessed transformative approaches that redefined its landscape. Pioneering

this shift, DLLP [1] employs deep networks to minimize the KL divergence between actual and predicted label proportions:

$$\mathcal{L}_{LLP}(\hat{\mathbf{p}}_k, \bar{\mathbf{p}}_k) = \sum_{c=1}^C \bar{p}_k^c \log \frac{\hat{p}_k^c}{\bar{p}_k^c} \quad (2)$$

where  $\hat{\mathbf{p}}_k = \frac{1}{m} \sum_{i=1}^m \mathbf{f}_\theta(\mathbf{x}_{ki})$  is the batch-averaged classification probability,  $\bar{p}_k^c$  is the true bag label proportion of class  $c$ ,  $C$  is the number of class,  $m$  is the bag size,  $x_{ki}$  is the  $i$ th instance in the bag  $k$ , and  $f_\theta(\cdot)$  is the instance-level classifier. This general LLP loss was adapted into a Cross-entropy form with an additional balanced Optimal Transport (OT) loss with entropic regularization by another study [15], signifying a move towards auxiliary loss functions and instance-level optimization for capturing label distributions [34]. However, as these LLP models grappled with scaling to larger bag sizes, LLP-VAT [55] attempted to mitigate this through consistency regularization and Virtual Adversarial Training [35], but still encountered the suboptimal issue, underscoring the ongoing struggle for *non-class-aware* supervision at the instance level. Diverging from these paths, LLP-GAN [33] championed the innovative GAN approach, melding generative adversarial techniques with LLP, a stride further propelled by LLP-AAE [62] through adversarial autoencoders. Meanwhile, models like LLP-Co [30] combined Contrastive learning with OT to ensure label proportion-guided clustering consistency across multi-views, and SELF-LLP [32] adopted Self-supervised techniques [18, 69] alongside the Self-ensemble strategy [31] to enhance representation robustness. Despite these methods have made significant advancements in the image, it reveals the gap in adapting these deep representation learning solutions to tabular data due to their reliance on image-specific techniques like label-invariant augmentation [30, 62] or universal pre-training paradigm [10]. This underscores the need for domain-agnostic solutions in LLP, especially for larger bag sizes and tabular data.

Recently, SelfCLR-LLP [37] introduced the first domain-agnostic contrastive learning framework aimed at the LLP challenge in tabular data. Leveraging an auxiliary Self-contrastive loss inspired by the NT-Xent loss [8], this method aims to enhance diversity without augmentation. However, a critical limitation is that the auxiliary loss overlooks label proportions, rendering the approach devoid of *class-awareness* at the instance level. Thus, it primarily enhances general-purpose representation diversity rather than providing a bespoke solution with class distinction for LLP, which risks sub-optimal performance in the face of poor dataset semantics and a black-box bagging scenario.

### 2.2 Contrastive Learning on Tabular Data.

Contrastive learning has become a potent Self-supervised learning paradigm in computer vision and natural language processing [13, 26, 57, 69], leveraging positive and negative pairs to optimize embedding spaces. Typical techniques like SimCLR [8] utilize data augmentations to create multiple views from single instances, employing InfoNCE loss [21, 40] for the learning process. This approach has also been adapted for supervised learning, shifting focus from homologous vs. non-homologous to class distinction [28]. However, applying contrastive learning to tabular data presents unique challenges due to low-quality data, lack of spatial correlations, and heterogeneity [5, 20]. Generating label-invariant views

or augmentations in tabular datasets requires preserving essential properties while introducing variation, a non-trivial task barely addressed through techniques like feature masking and random manipulation [64, 65]. VIME [65] capitalizes on corruption techniques tailored for tabular data and introduces a consistency loss. This corruption concept has later extended to contrastive learning by SCARF [3] based on empirical distributions. SAINT [47] further combines contrastive learning with denoising reconstruction, integrating feature mixup augmentation [68, 70]. However, the mixed nature of tabular data, along with issues like significant predictive power held by individual features, makes any form of data manipulation or augmentation a sensitive operation [46]. Recent works propose to subset the raw features [58] to tackle these challenges, but generating strong and intact augmentations for Contrastive learning, even in fully supervised scenarios, remains a challenge.

### 3 METHODOLOGY

#### 3.1 Motivational Study and Overview

**3.1.1 Inherent LLP Difficulty.** As introduced in Sec.1, a pivotal LLP difficulty is the inherent ambiguity when multiple instance label combinations within a bag yield identical label proportions [30], leading to a misalignment between bag-level training objectives and instance-level predictions. This discrepancy hinders the model’s ability to classify individual instances from aggregated data.

The concavity of the logarithm function implies, according to Jensen’s Inequality [24], that for a concave function  $f$  and a random variable  $X$ ,  $f(\mathbb{E}[X]) \geq \mathbb{E}[f(X)]$ . Applying this principle to the LLP loss highlights a critical insight. Given the instance-level classification formulated as the cross-entropy loss:

$$\mathcal{L}_{\text{Ins}}(\hat{y}, y) = -\frac{1}{m} \sum_{i=1}^m \sum_{c=1}^C y_i^c \log \hat{y}_i^c \quad (3)$$

where  $y_i^c$  is the true label of instance  $i$  for class  $c$ , and  $\hat{y}_i^c = f_\theta(x_i)^c$  is the predicted probability of instance  $i$  belonging to class  $c$ . We observe that  $\mathcal{L}_{\text{LLP}}$ ’s logarithm of the average prediction  $\log(\mathbb{E}[X])$  is greater than or equal to  $\mathcal{L}_{\text{Ins}}$ ’s average of the logarithms of individual predictions  $\mathbb{E}(\log[X])$ . This mathematical exposition underscores a fundamental gradient suboptimality [28] of relying solely on bag-level loss functions, such as LLP loss [1, 15], for optimizing instance-level predictions. While such an approach may align the model’s average predictions with the true label proportions across bags, it does not inherently guarantee the precision of predictions for each instance within those bags. Ensuring models achieve both aggregate accuracy and instance-level precision requires strategies that directly address the optimization of individual instance predictions within the LLP framework.

**3.1.2 Tabular-based LLP Problem Formulation.** We defined the tabular LLP Problem addressed by TabLLP-BDC as:

**DEFINITION 1 (TABLLP-BDC’S TABULAR-BASED LLP PROBLEM).** Given an instance-level classifier in deep tabular learning that consists of an encoder  $f_\theta$ , projection head  $g_\delta$ , prediction head  $h_\omega$ , a tabular LLP dataset  $D_{\text{LLP}} = \{(B_k, \bar{p}_k)\}_{k=1}^K$ , and loss weights  $\alpha, \beta, \lambda, \gamma$ , the

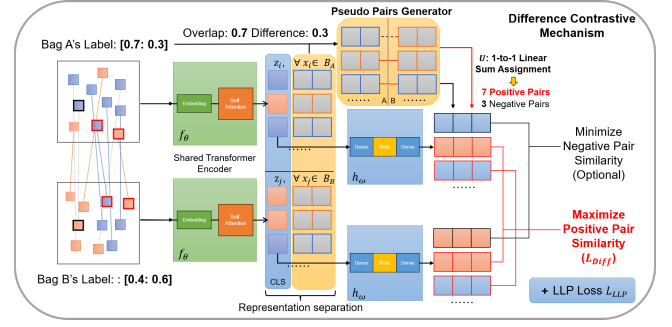


**Figure 1: Overview of TabLLP-BDC’s Difference Contrastive Mechanism.** Consider the optimal mapping between two instance bags, colored lines represent potential positive samples, and dashed lines represent negative samples. The figure shows the forward process of two positive sample pairs marked in red and one negative sample pair marked in black.

definition of TabLLP-BDC is formally formulated as:

$$\begin{aligned} \theta_{\text{init}}, \delta^* &= \arg \min_{\theta, \delta} [\alpha \mathcal{L}_{\text{Bag}}(g_\delta(f_\theta(B)), \bar{p}) + \beta \mathcal{L}_{\text{Self}}(g_\delta(f_\theta(B)))], \\ \theta^*, \omega^* &= \arg \min_{\theta_{\text{init}}, \omega} [\lambda \mathcal{L}_{\text{Diff}}(f_\theta(B), \bar{p}) + \gamma \mathcal{L}_{\text{LLP}}(h_\omega(f_\theta(B)), \bar{p})], \end{aligned}$$

where  $\mathcal{L}_{\text{Bag}}(\cdot, \cdot)$  denotes our Bag Contrastive pretraining loss,  $\mathcal{L}_{\text{Self}}(\cdot)$  denotes the classical Self-contrastive + Denoising Reconstruction pre-training loss,  $\mathcal{L}_{\text{Diff}}(\cdot, \cdot)$  denotes our instance-level Difference Contrastive loss, and  $\mathcal{L}_{\text{LLP}}(\cdot, \cdot)$  denotes the classical bag-level LLP loss.

Compared to classical LLPs, the novelty of TabLLP-BDC includes:

- An instance-level, *class-aware* fine-tuning strategy  $\mathcal{L}_{\text{Diff}}(\cdot, \cdot)$  on the encoded representation  $f_\theta(B)$  to bridge the gap between bag-level training ( $\mathcal{L}_{\text{LLP}}(\cdot, \cdot)$ ) and instance-level prediction.
- A bag-level pretraining strategy  $\mathcal{L}_{\text{Bag}}(\cdot, \cdot)$  on top of the projection  $g_\delta(f_\theta(B))$  to ensure intrinsic tabular feature correlations captured by  $\mathcal{L}_{\text{Self}}(\cdot)$  comply with label proportion distribution.

Algo. 1 presents the procedure of two-stage training. Both stages are favorable for tabular data by relying on bag comparison, thus achieving augmentation-free, and leveraging label proportion to establish contrastive signals, thus achieving *class-aware*. See Appx. A.2, Fig. 1, and 4 for the detailed model architecture.

#### 3.2 Difference Contrastive Finetuning

Based on the theoretical insights into the inherent LLP difficulty (Sec. 3.1.1), we propose a Difference Contrastive mechanism to augment the missing instance-level supervision that arises when relying solely on bag-level finetuning loss  $\mathcal{L}_{\text{LLP}}(\cdot, \cdot)$ . This method is anchored on an inherent property of label proportion observed during multi-bag comparisons. Given an optimal encoder  $f_\theta^*$  and two bags of instances with label proportion  $\bar{p}_1$  and  $\bar{p}_2$ , there exists an optimal 1-to-1 mapping assignment between the instance representations from different bags, forming  $n_{\text{pos}} = m \sum_{c=0}^C \min(\bar{p}_1^c, \bar{p}_2^c)$  positive pairs of the same label and  $n_{\text{neg}} = m - n_{\text{pos}}$  negative pairs of different labels (depicted in Fig. 1).

Formally, for two bags of samples, each of size  $n$ , and a similarity matrix  $S$  where  $S_{ij}$  represents the cosine similarity between the  $i$ -th sample of the first bag and the  $j$ -th sample of the second, the

optimal assignment aims to determine the positive pairs set  $P$  and the negative pairs set  $Q$  to maximize the given formula:

$$\begin{aligned} O(S, n_{\text{pos}}) &= \max_{P, Q} \left( \sum_{(i,j) \in P} S_{ij} + \sum_{(i,j) \in Q} -S_{ij} \right) \\ \text{s.t. } |P| &= n_{\text{pos}}, |Q| = m - n_{\text{pos}}, \\ U &= P \cup Q \text{ is a 1-to-1 linear assignment.} \end{aligned}$$

The resulting positive and negative pairs can then be used as pseudo-labels to train the model with the Cosine Embedding loss to encourage positive pairs to have similar representation and vice versa. Unfortunately, this problem is inherently combinatorial, and cannot be solved by a computationally efficient algorithm. A notable exception arises when two bags have identical label proportions. In such a case,  $n_{\text{pos}} = m$  and no negative pairs exist, the formula can therefore be simplified as:

$$\begin{aligned} O(S) &= \max_U \sum_{(i,j) \in U} S_{ij} \\ \text{s.t. } U &\text{ is a 1-to-1 linear assignment.} \end{aligned}$$

This is known as the Linear Sum Assignment problem and can be solved by the Hungarian Algorithm [9] in polynomial time. By removing the explicit consideration of negative pairs, this method yields a good approximation of our combinatorial problem.

Therefore, given the positive pairs generated by selecting the Top- $n_{\text{pos}}$  similarity 1-to-1 pairs after adopting the Hungarian Algorithm, we propose the Difference Contrastive Loss as follows:

$$\mathcal{L}_{Diff}(Z, P) = \frac{1}{|P|} \sum_{(i,j) \in P} -\log \frac{\exp(\cos(z_i, z_j)/\tau)}{\sum_{k \in \text{another bag}} \exp(\cos(z_i, z_k)/\tau)} \quad (4)$$

where  $z_i \in Z$  is the instance representation,  $(i, j)$  is a positive pair from  $P$ ,  $\cos$  is the cosine similarity, and  $k$  is any sample from the other bag including  $j$ . This Difference Contrastive Loss utilizes the pseudo-pairs generated based on the difference in two bags' label proportions, serving as an intermediary between the classical Self-contrastive loss [8] and the Supervised Contrastive loss [28]. In contrast to the NT-Xent loss, which is typically employed as the Self-contrastive loss, our approach shifts the contrastive objective from determining if representations originate from the same sample to discerning if they belong to the same class, which is, therefore, *class-aware*. This adjustment not only integrates instance-level supervision with *class-aware* guidance into the LLP task but also obviates the need for label-invariant augmentation to produce varied views of instances. All instances from the opposite bag of anchor instances  $z_i$  are treated as negative pairs because of the inherent 1-to-1 mapping constraint and the approximation assumption.

The overall finetuning loss is defined in a multi-task fashion as a ramp-down LLP Loss and a ramp-up Difference Contrastive Loss:

$$\begin{aligned} \mathcal{L} &= \lambda(t) \mathcal{L}_{Diff}(Z, P) + \gamma(t) \mathcal{L}_{LLP}(\hat{p}, \bar{p}) \\ &= \lambda(t) \frac{1}{|P|} \sum_{(i,j) \in P} -\log \frac{\exp(\cos(z_i, z_j)/\tau)}{\sum_{k \in \text{another bag}} \exp(\cos(z_i, z_k)/\tau)} \\ &\quad + \frac{\gamma(t)}{2} \left[ \sum_{c=1}^C \bar{p}_1^c \log \frac{\bar{p}_1^c}{\hat{p}_1^c} + \sum_{c=1}^C \bar{p}_2^c \log \frac{\bar{p}_2^c}{\hat{p}_2^c} \right] \end{aligned} \quad (5)$$

where  $\lambda(t) = \exp\left(-5 \times \left(1 - \frac{t}{T}\right)^2\right)$  and  $\gamma(t) = 1 - \lambda(t)$  are the exponential ramp-up and ramp-down weight at epoch  $t$  over  $T$ .  $\mathcal{L}_{LLP}(\cdot, \cdot)$  serves as an initiator for learning an optimal classifier  $f_\theta^*$ , aiming at generating pseudo-positive pairs more accurately.

### 3.3 Bag Contrastive Pretraining

Learning from Label Proportion (LLP), like other subareas of WSL, holds significant potential for pretraining. By capturing feature correlations before being supervised by ambiguous weak labels, the model is less likely to converge to suboptimal solutions [56]. Despite its potential, the exploration of pretraining specifically for tabular-based LLP framework remains untouched, likely due to the dominant emphasis on image, where many universal pretraining models exist [10]. In order to fill this gap, we first adopted a proven unsupervised pre-training pipeline in the field of deep tabular learning, termed this approach ‘‘Self-contrastive pretraining.’’ As detailed in the Appx. A.3, this instance-level method harmonizes MixUp [70] and CutMix [68] augmentations with Self-contrastive and denoising reconstruction to enhance pretraining efficacy [47].

However, empirical studies in Tab. 7 reveal that such a pretraining approach may occasionally underperform compared to scenarios devoid of pretraining within the LLP context, highlighting its unpredictable effectiveness. To mitigate this discrepancy between instance-level pretraining and bag-level learning, we propose the Bag Contrastive pretraining task. This innovation ensures that the Self-contrastive pretraining process [3, 47] aligns with the variations in label proportions at the bag level, thereby nurturing suitable sample representations for subsequent fine-tuning tasks. Drawing inspiration from the attention mechanism—particularly intersample attention [47, 59]—alongside classical MIL aggregation methods [23], we advocate a bag aggregator to compute the weighted sum of instance embeddings within a bag, where weights are determined by intersample similarity through a query network:

$$\mathbf{b} = \text{softmax}\left(\mathbf{Z}\mathbf{W}\mathbf{Z}^T\right)\mathbf{Z} \quad (6)$$

where  $\mathbf{Z}$  is the matrix of instance representations in a bag,  $\mathbf{W}$  denotes the weight matrix of the query network, and  $\mathbf{b}$  is the aggregated bag representation. This aggregation adeptly computes the bag representation [23], and the contribution of each sample to the bag representation is determined by its relation with other samples within the same bag, implicitly reflecting the bag label proportion. To instill reliable bag-level labels, we design the Bag Contrastive task along the principles of deep metric learning [27]:

$$\begin{aligned} \mathcal{L}_{Bag}(\mathbf{b}, \bar{\mathbf{p}}) &= (1 - \text{mPIoU}(\bar{\mathbf{p}}_1, \bar{\mathbf{p}}_2)) \cdot \max(0, \cos(\mathbf{b}_1, \mathbf{b}_2) - \text{margin}) \\ &\quad + \text{mPIoU}(\bar{\mathbf{p}}_1, \bar{\mathbf{p}}_2) \cdot (1 - \cos(\mathbf{b}_1, \mathbf{b}_2)). \end{aligned} \quad (7)$$

Here,  $\bar{\mathbf{p}}_1$  is the label proportion of the first bag,  $\mathbf{b}_2$  is the bag representation of the second bag, mPIoU symbolizes our proposed mean proportion intersection over union metric between two bags (details in Sec. 4.1.3), while  $\cos$  signifies the cosine similarity between the two bag representations. Alternative metrics like L1 can substitute mPIoU without notable performance deviations, and the efficacy of our proposed bag-level metric is explored in the Appx. D.5. Collectively, the Bag Contrastive loss encourages that the model's representations are consistent with the label proportions, guiding the pretraining toward more reliable embeddings.

**Table 2: Fine-grained Experimental Results.**

	AUC (%)							Accuracy (%)	
	AD	BA	CA	CR	EL	RO	ML	Private A	Private B
Supervised	91.37 ± 0.20	94.01 ± 0.18	95.87 ± 0.08	82.36 ± 0.07	90.73 ± 0.15	89.48 ± 0.05	86.02 ± 0.1	60.02 ± 1.54	86.77 ± 0.40
DLLP	87.61 ± 0.21	77.18 ± 1.07	78.75 ± 1.50	75.07 ± 0.58	74.33 ± 0.71	79.10 ± 0.19	73.75 ± 0.81	50.39 ± 0.18	68.86 ± 2.63
LLP-GAN	83.60 ± 1.25	72.06 ± 2.45	83.05 ± 0.55	75.90 ± 1.07	56.75 ± 3.74	74.44 ± 0.40	74.31 ± 1.52	50.14 ± 0.15	66.77 ± 4.14
LLP-VAT	86.76 ± 0.25	81.19 ± 2.03	79.99 ± 2.17	74.93 ± 0.45	74.34 ± 0.76	79.09 ± 0.22	71.12 ± 1.20	49.47 ± 0.39	73.62 ± 0.93
SelfCLR-LLP	87.44 ± 0.22	79.73 ± 1.51	81.34 ± 2.11	75.43 ± 0.34	74.44 ± 0.81	78.97 ± 0.30	74.36 ± 1.31	50.28 ± 0.24	68.99 ± 2.88
TabLLP-DEC	62.62 ± 3.35	70.24 ± 1.53	81.61 ± 0.32	76.27 ± 0.42	73.71 ± 2.47	72.68 ± 0.44	55.34 ± 0.50	49.77 ± 0.04	55.70 ± 3.39
TabLLP-PSE	87.64 ± 0.29	80.26 ± 1.67	79.73 ± 1.85	77.53 ± 0.72	75.42 ± 1.91	79.06 ± 0.10	74.18 ± 0.36	50.48 ± 0.13	70.37 ± 1.17
TabLLP-SELF	86.66 ± 0.38	79.38 ± 0.90	82.55 ± 0.74	77.04 ± 0.97	74.87 ± 0.78	79.19 ± 0.28	74.10 ± 0.79	50.41 ± 0.28	66.60 ± 1.64
<b>TabLLP-BDC</b>	<b>87.81 ± 0.18</b>	<b>84.95 ± 1.88</b>	<b>84.85 ± 0.93</b>	<b>79.29 ± 0.39</b>	<b>77.53 ± 1.48</b>	<b>79.67 ± 0.25</b>	<b>75.06 ± 0.58</b>	<b>51.39 ± 0.16</b>	<b>74.03 ± 1.54</b>

## 4 EXPERIMENTS

### 4.1 Experimental Settings

**4.1.1 Datasets, preprocessing, and bagging.** Our major study utilizes seven datasets: seven public tabular datasets sourced from OpenML<sup>1</sup> and a private dataset from the gaming industry. These public datasets, renowned in literature as classical binary classification datasets, each comprise at least 15,000 instances, aligning with the large-scale and black-box scenario of LLP. The private dataset, encompassing in-game behaviors of over 300,000 players, aims to deduce multi-class gamer demographics. Labels for this dataset are exclusively available in a bag label proportion format from an advertising platform, with a constraint of a minimum of 250 distinct instances per bag. We employ the same preprocessing standards as related works [3, 20, 47] and advocate an ordered bagging strategy for scalability and label diversity. Details of dataset statistics (Tab. 8), preprocessing techniques, and comparison of bagging strategies (Fig. 5 and Tab. 9) are discussed in the Appx. B.1 and B.2.

**4.1.2 Baselines.** Given the nascent exploration of LLP in tabular data, we adapt several leading LLP image data baselines and introduce intuitive model ideas for pure tabular scenarios. Notably, direct adaptations of some image data baselines may not be feasible due to tabular data’s distinct characteristics, so our selection prioritizes methods that are easily transferable. The list of comparing baselines includes: DLLP [1] (fundamental LLP loss), LLP-GAN [33] (superior GAN-based model in the image domain), LLP-VAT [55] (classical consistency regularization work in the image domain), SelfCLR-LLP [37] (the only work addressing deep LLP in the tabular domain), TabLLP-DEC (intuitive adaptation of classical Deep Clustering model [63] with LLP constrain), TabLLP-PSE (intuitive pseudo-labeling with constrained KMeans, similar to [34]), and TabLLP-SELF (intuitive contrastive variant inspired from SelfCLR-LLP [37] but with typical augmentation technique for tabular data [47, 65, 68, 70]). The details of necessary modification and reasons for selection are discussed in the Appx. B.4.

**4.1.3 Evaluation Methods.** Consistent with prevalent practices [1, 33, 37, 55], our primary evaluation metrics are the AUC score for binary classification and Accuracy for multi-class classification. Recognizing the inherent difficulty of LLP evaluations without instance-level labels, we employ the L1 as an alternative metric

[55]. Additionally, we propose the mean Proportional-Intersection-Over-Union (mPIoU) metric, inspired by semantic segmentation’s mIoU metric. Given  $\hat{p}^c$  as the predicted label proportion for class  $c$ ,  $p^c$  as the true label proportion for class  $c$ , and  $C$  as the number of classes for which the union is non-zero, the mPIoU is defined as:  $mPIoU = \frac{1}{C} \sum_{c=1}^C \frac{\min(\hat{p}^c, p^c)}{\max(\hat{p}^c, p^c)}$ . This metric evaluates the congruence between predicted and actual label proportions across classes. The metric’s efficacy is further discussed in the Tab. 19 and Appx. D.5.

**4.1.4 Model Implementation and Training Setting.** The SAINT-s model [47] is our default encoder for tabular data. We undergo 50 epochs in pretraining and 300 in finetuning, with a 20-epoch early stopping based on validation scores. Hyperparameters are optimized using Optuna<sup>2</sup> across 50 trials for each dataset and model, and we repeat 10 trials per experiment with varied seeds. Further details and component analysis are discussed in the Appx. B.3.

### 4.2 Experimental Results

Our comprehensive experimental evaluation demonstrates the superior performance of TabLLP-BDC against a wide range of LLP baselines across various validation set granularities and bag sizes. For consistency and relevance to practical applications, experiments default to a bag size of 256. Detailed insights into the components’ contributions are further explored in the Sec. 4.3 and Appx. D.

**4.2.1 Performance Evaluation with Fine-grained Validation.** This section delves into a common LLP setup featuring accessible fine-grained validation, aligning with evaluations in prior works [1, 33, 34, 37, 55]. Tab. 2 presents AUC scores for binary datasets and accuracy for multi-class datasets, where TabLLP-BDC exhibits consistent superiority over other LLP classifiers. This advantage is attributed to our novel approach combining Bag Contrastive pretraining and Difference Contrastive fine-tuning, which fosters *class-aware* and instance-specific learning. As discussed in Sec.4.2.3, unlike methods such as SelfCLR-LLP [37] and TabLLP-SELF, which lack *class-awareness*, TabLLP-BDC explicitly ensures instances of the same class are represented similarly.

**4.2.2 Performance Evaluation with Coarse-grained Validation.** Addressing a more challenging scenario devoid of fine-grained validation, often restricted by privacy considerations [12], this practical

<sup>1</sup><https://www.openml.org/>

<sup>2</sup><https://optuna.org/>



**Table 3: The Class Awareness Score (CAS) is calculated based on the standardized intra-class and inter-class similarity in the representation space, with higher scores indicating higher *class-awareness*. The highest score for each class is **bolded**, while the second highest is underlined.**

Model	Class Awareness Score (CAS)				
	AD	BA	CA	CR	EL
DLLP	<b>0.8223</b>	<u>0.5208</u>	0.5192	<u>0.8251</u>	0.5008
SelfCLR-LLP	0.5461	0.5167	<u>0.5446</u>	0.6090	0.5005
TabLLP-SELF	0.5080	0.5013	0.5160	0.5719	<u>0.5103</u>
TabLLP-BDC	<u>0.6176</u>	<b>0.6329</b>	<b>0.5802</b>	<b>0.9514</b>	<b>0.5104</b>

**Table 4: The Accuracy of Pseudo-pairs Generator.**

Scenario	Accuracy (%)				
	AD	BA	CA	CR	EL
Fine-grained	<b>78.1</b>	<b>85.9</b>	<b>63.8</b>	<b>61.7</b>	<b>67.4</b>
Coarse-grained	77.0	84.9	60.4	60.2	65.8

analysis validates models' performance based on bag label proportions, implementing early stopping based on L1 scores or our mPIoU metric. Our results, displayed in Tab. 12 (Appx.C), reiterate TabLLP-BDC's lead in performance, albeit with some variations in mPIoU or L1 scores. These fluctuations underscore the complex nature of tabular data, characterized by limited semantics and prevalent noise [5, 20]. The imperfect correlation between the best instance-level predictions and label proportions, as shown in Tab. 13 (Appx.C), validates our hypothesis that solely relying on bag-level loss is insufficient for accurate instance-level prediction in tabular data.

**4.2.3 Verification of Class Awareness.** We assess class awareness in the representation space, introducing the Class Awareness Score (CAS). This metric, reflecting the ratio of standardized intra-class to the sum of standardized intra-class and inter-class cosine similarities, gauges the discriminative capacity of representations. TabLLP-BDC, as depicted in Tab. 3, exhibits superior discriminative capabilities over the three most potent baselines lacking class awareness across five medium-sized datasets. This underscores the value of *class-aware* supervision in generating distinct and robust class representations. Notably, although DLLP also achieves good CAS, its intra-class and inter-class similarities are very low, which reflects the inherent ambiguity of label proportion matching.

**4.2.4 Effectiveness of Pseudo Pair Generator.** We explore the precision of pseudo-positive pair generation in the Difference Contrastive fine-tuning without reliance on granular labels. Tab. 4 reveals that pseudo-positive pairs, derived from label proportion comparisons, achieve notable accuracy. Unlike simple nearest-neighbor pairings, the Linear Sum Assignment method introduces appropriate difficulty to pair generation, occasionally impacting accuracy but fostering more discriminative and class-congruent representations. This strategic trade-off, as empirically validated in Tab. 15 (Appx.D.2) against the nearest-neighbor pairings, culminates in an uplift in overall model performance.

**4.2.5 Influence of Bag Size.** We examine the impact of varying bag sizes on the LLP framework, prioritizing larger sizes to reflect

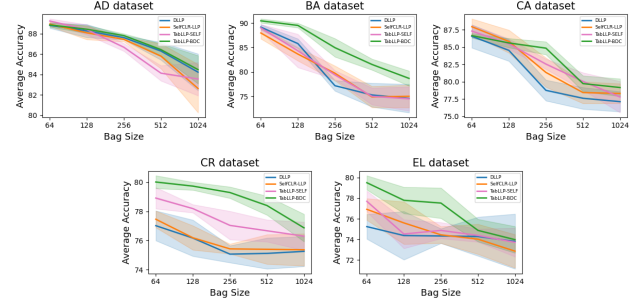


**Figure 2: The impact of varying bag sizes on four most potent models across five medium size datasets.**

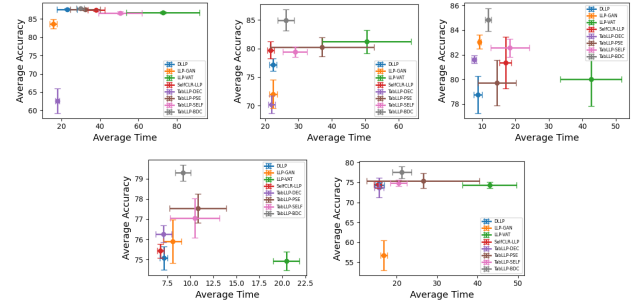


**Figure 3: Accuracy-vs-Time diagrams.**

industry-scale applications: {64, 128, 256, 512, 1024}. Fig. 2 illustrates the performance trends and variability of the three most potent baselines within contrastive learning frameworks alongside TabLLP-BDC. Consistent with prior research [1, 33, 34, 37, 55], prediction accuracy approaches that of supervised learning as bag sizes decrease. Nonetheless, their performance drops markedly with larger bags. Contrary to the sharp performance decline noted in image data LLP studies, tabular-based LLP models, especially our TabLLP-BDC, demonstrate robust adaptability to larger bag sizes, underscoring the promising potential in practical settings.

**4.2.6 Model Robustness.** We conducted a robustness ranking of various models by analyzing their performance standard deviation across multiple datasets, as detailed in Tab. 5. This ranking system, assigning scores from 1 (most stable) to 8 (least stable) based on standard deviation, serves to quantify each model's stability across diverse scenarios. The overall robustness ranking, derived from averaging these scores, positions TabLLP-BDC as the second most stable model, showcasing its consistent performance. Although DLLP exhibits the highest stability, its model performance across datasets does not match that of TabLLP-BDC. Additionally, the Accuracy-vs-Time diagram for all models, illustrated in Fig. 3, demonstrates TabLLP-BDC's balanced trade-off between accuracy and training time, reinforcing its robustness.

**4.2.7 Training Time Analysis.** Tab. 6 presents an evaluation of the training efficiency for various models, highlighting both the average training duration and its variability. This analysis is crucial for gauging each model's computational demands, a key consideration for their deployment in environments with limited resources. For the five medium-sized datasets, TabLLP-BDC achieves Top 2 efficiency in four instances, indicating a remarkable compromise

**Table 5: Average robustness ranking for each model.**

Model	Average Robustness Ranking
DLLP	3.375
LLP-GAN	6.375
LLP-VAT	4.625
SelfCLR-LLP	4.5
TabLLP-DEC	4.875
TabLLP-PSE	4.125
TabLLP-SELF	4.5
TabLLP-BDC	3.625

**Table 6: Average training time and standard deviation.**

Model	Avg. (std) Training Time (min)				
	AD	BA	CA	CR	EL
DLLP	22.86(5.28)	22.35(1.11)	8.76(1.30)	7.09(0.44)	15.68(1.14)
LLP-GAN	22.50(2.50)	22.45(1.10)	9.30(0.34)	8.04(1.00)	16.80(0.82)
LLP-VAT	72.80(19.03)	50.49(13.24)	42.58(9.22)	20.43(1.42)	42.98(6.73)
SelfCLR	38.06(4.35)	21.66(0.96)	17.01(1.84)	6.73(0.37)	15.29(0.90)
DEC	17.87(1.16)	21.98(1.05)	7.66(0.67)	7.07(0.86)	15.65(1.16)
PSE	32.35(7.66)	37.06(15.57)	14.44(5.69)	10.82(3.08)	26.55(13.95)
SELF	50.64(11.23)	28.97(3.65)	18.39(5.73)	10.46(2.69)	20.44(2.06)
BDC	22.23(2.01)	20.02(2.44)	9.19(0.97)	6.83(0.86)	12.69(2.34)
Pretrain	7.64(0.13)	6.20(0.82)	2.68(0.15)	2.36(0.15)	8.57(0.90)

between computational time and performance enhancement. Although the inclusion of a pretraining phase marginally extends the training period, the consistent performance gains across models justify this additional investment. Consequently, TabLLP-BDC emerges as a cost-effective solution for tackling the tabular-based LLP challenge, given its superior accuracy and efficiency.

### 4.3 Ablation Study

We present a comprehensive ablation study to assess the individual and combined effect of the components within our TabLLP-BDC model in the Appx. D. Here is a summary of the main findings:

- **Ablation Study of Downstream Contrastive Objectives:** The Difference Contrastive objective consistently outperforms other contrastive-based objectives across most scenarios and datasets and achieves solid SOTA when combined with the best pretraining task. (Tab. 14 in Appx. D.1)
- **Ablation Study of Downstream Components:** The Linear Sum Assignment method for generating pseudo-positive pairs (Tab. 15), combined with the Supervised InfoNCE-based Contrastive loss (Tab. 16), provides the best balance between performance and efficiency compared to Greedy Pairwise Assignment and Cosine Embedding loss. (Appx. D.2)
- **Ablation Study of Pretraining Tasks:** Our pretraining strategy, including the Bag Contrastive task, effectively bridges instance-level pretraining and bag-level finetuning, consistently enhancing the performance of several tabular LLP models. However, combining Bag Contrastive with Difference Contrastive may not always amplify each other's benefits, suggesting potential overlaps. (Tab. 7 and Appx. D.3)
- **Ablation Study of Pretraining Components:** Separating representation by the CLS token is an augmentation-free and more efficient alternative to the typical sample manipulation, e.g., feature mixup, when augmenting tabular data (Tab. 17). In terms of aggregation techniques (Tab. 18), the similarity-driven weighted sum aggregator generally outperforms the intersample attention-based aggregator both with and without the projector. (Appx. D.4)

**Table 7: Ablation Study of Pretraining Tasks.**

Pretrain	Model	AUC (%)				
		AD	BA	CA	CR	EL
No	DLLP	87.64	77.18	78.75	75.07	74.33
Self	DLLP	87.55	<b>84.36</b>	83.53	75.58	75.31
Bag	DLLP	87.71	81.57	83.28	<b>75.60</b>	74.82
Self+Bag	DLLP	<b>87.76</b>	82.63	<b>84.40</b>	75.51	<b>75.64</b>
No	SelfCLR	87.44	79.73	81.34	75.43	74.44
Self	SelfCLR	87.51	<b>83.50</b>	84.41	75.85	75.26
Bag	SelfCLR	87.49	79.05	84.27	75.51	75.14
Self+Bag	SelfCLR	<b>87.67</b>	81.69	<b>84.78</b>	<b>76.13</b>	<b>75.40</b>
No	SELF	86.66	79.38	82.55	77.04	74.87
Self	SELF	86.63	<b>83.16</b>	84.04	77.09	75.22
Bag	SELF	86.50	77.71	82.92	77.34	75.28
Self+Bag	SELF	<b>86.99</b>	82.78	<b>84.19</b>	<b>77.69</b>	<b>75.44</b>
No	BDC	87.03	81.77	80.64	79.10	75.43
Self	BDC	87.79	<b>84.95</b>	<b>84.85</b>	<b>79.29</b>	76.24
Bag	BDC	87.80	84.06	83.12	78.59	75.82
Self+Bag	BDC	<b>87.81</b>	84.91	83.94	79.16	<b>77.53</b>

- **Evaluation of Bag-Level Metrics in Early Stopped LLP Models:** Both the L1 metric and the proposed mPIoU metric offer valuable insights, but the mPIoU metric provides a more nuanced evaluation, suggesting its potential for a more comprehensive assessment in future research. (Tab. 19 in Appx. D.5)

## 5 CONCLUSION

In this study, we addressed the intricate challenges of Learning from Label Proportions (LLP) with a focus on tabular data. Our innovative TabLLP-BDC model introduces a *class-aware* and augmentation-free contrastive learning framework tailored for tabular-based LLP. This approach effectively bridges the gap between bag-level supervision and the desired instance-level predictions, overcoming the unique hurdles of generating *class-aware* and augmentation-free instance-level signals for tabular data. The model's design is underpinned by two key mechanisms: Bag Contrastive pretraining and Difference Contrastive fine-tuning. Together, these elements enable our model to leverage detailed instance-level insights while adhering to holistic bag-level cues. Additionally, our work introduces the mPIoU metric, specifically designed for bag-level validation, enhancing the robustness of our evaluation process and underscoring the practical utility of our model. Empirical validations across various datasets demonstrate TabLLP-BDC's outstanding performance, proving its versatility and efficacy, particularly in user modeling and personalization applications. Looking ahead, this research paves the way for further advancements in pseudo-pair generation techniques based on label proportion comparisons and aims to refine our objectives to better extract and utilize the latent instance-level insights embedded within label proportions.



## REFERENCES

- [1] Ehsan Mohammady Ardehaly and Aron Culotta. 2017. Co-training for demographic classification using deep learning from label proportions. In *2017 IEEE International Conference on Data Mining Workshops (ICDMW)*. IEEE, 1017–1024.
- [2] Ricardo Baeza-Yates, Di Jiang, Fabrizio Silvestri, and Beverly Harrison. 2015. Predicting the next app that you are going to use. In *Proceedings of the eighth ACM international conference on web search and data mining*. 285–294.
- [3] Dara Bahri, Heinrich Jiang, Yi Tay, and Donald Metzler. 2021. Scarf: Self-supervised contrastive learning using random feature corruption. *arXiv preprint arXiv:2106.15147* (2021).
- [4] Emanuel Bayer, Shuba Srinivasan, Edward J Riedl, and Bernd Skiera. 2020. The impact of online display advertising and paid search advertising relative to offline advertising on firm performance and firm value. *International Journal of Research in Marketing* 37, 4 (2020), 789–804.
- [5] Vadim Borisov, Tobias Leemann, Kathrin Seßler, Johannes Haug, Martin Pawelczyk, and Gergely Kasznci. 2022. Deep neural networks and tabular data: A survey. *IEEE Transactions on Neural Networks and Learning Systems* (2022).
- [6] Mathilde Caron, Piotr Bojanowski, Armand Joulin, and Matthijs Douze. 2018. Deep clustering for unsupervised learning of visual features. In *Proceedings of the European conference on computer vision (ECCV)*. 132–149.
- [7] Shuo Chen, Bin Liu, Mingjie Qian, and Changshui Zhang. 2009. Kernel k-means based framework for aggregate outputs classification. In *2009 IEEE International Conference on Data Mining Workshops*. IEEE, 356–361.
- [8] Ting Chen, Simon Kornblith, Mohammad Norouzi, and Geoffrey Hinton. 2020. A simple framework for contrastive learning of visual representations. In *International conference on machine learning*. PMLR, 1597–1607.
- [9] David F Crouse. 2016. On implementing 2D rectangular assignment algorithms. *IEEE Trans. Aerospace Electron. Systems* 52, 4 (2016), 1679–1696.
- [10] Jia Deng, Wei Dong, Richard Socher, Li-Jia Li, Kai Li, and Li Fei-Fei. 2009. Imagenet: A large-scale hierarchical image database. In *2009 IEEE conference on computer vision and pattern recognition*. Ieee, 248–255.
- [11] Facebook Developers. 2023. View aggregated data for your campaigns, ad sets or ads in Meta Ads Manager. <https://www.facebook.com/business/help/235326303504525> Accessed: 2023-9-22.
- [12] Google Developers. 2023. Privacy checks in Ads Data Hub. <https://developers.google.com/ads-data-hub/guides/privacy-checks> Accessed: 2023-9-22.
- [13] Jacob Devlin, Ming-Wei Chang, Kenton Lee, and Kristina Toutanova. 2018. Bert: Pre-training of deep bidirectional transformers for language understanding. *arXiv preprint arXiv:1810.04805* (2018).
- [14] Yutao Dong, Qing Li, Richard O Sinnott, Yong Jiang, and Shutao Xia. 2021. ISP self-operated BGP anomaly detection based on weakly supervised learning. In *2021 IEEE 29th International Conference on Network Protocols (ICNP)*. IEEE, 1–11.
- [15] Gabriel Dulac-Arnold, Neil Zeghidour, Marco Cuturi, Lucas Beyer, and Jean-Philippe Vert. 2019. Deep multi-class learning from label proportions. *arXiv preprint arXiv:1905.12909* (2019).
- [16] Justin Engelmann and Stefan Lessmann. 2021. Conditional Wasserstein GAN-based oversampling of tabular data for imbalanced learning. *Expert Systems with Applications* 174 (2021), 114582.
- [17] X Yu Felix, Dong Liu, Sanjiv Kumar, Tony Jebara, and Shih-Fu Chang. 2013. PSVM for learning with label proportions. (2013).
- [18] Spyros Gidaris, Praveer Singh, and Nikos Komodakis. 2018. Unsupervised representation learning by predicting image rotations. *arXiv preprint arXiv:1803.07728* (2018).
- [19] Yury Gorishniy, Ivan Rubachev, Valentin Khrukov, and Artem Babenko. 2021. Revisiting deep learning models for tabular data. *Advances in Neural Information Processing Systems* 34 (2021), 18932–18943.
- [20] Léo Grinsztajn, Edouard Oyallon, and Gaël Varoquaux. 2022. Why do tree-based models still outperform deep learning on typical tabular data? *Advances in Neural Information Processing Systems* 35 (2022), 507–520.
- [21] Michael Gutmann and Aapo Hyvärinen. 2010. Noise-contrastive estimation: A new estimation principle for unnormalized statistical models. In *Proceedings of the thirteenth international conference on artificial intelligence and statistics*. JMLR Workshop and Conference Proceedings, 297–304.
- [22] Jerónimo Hernández-González, Inaki Inza, and Jose A Lozano. 2013. Learning Bayesian network classifiers from label proportions. *Pattern Recognition* 46, 12 (2013), 3425–3440.
- [23] Maximilian Ilse, Jakub Tomczak, and Max Welling. 2018. Attention-based deep multiple instance learning. In *International conference on machine learning*. PMLR, 2127–2136.
- [24] Johan Ludwig William Valdemar Jensen. 1906. Sur les fonctions convexes et les inégalités entre les valeurs moyennes. *Acta mathematica* 30, 1 (1906), 175–193.
- [25] Minqi Jiang, Chaochuan Hou, Ao Zheng, Xiyang Hu, Songqiao Han, Hailiang Huang, Xiangnan He, Philip S Yu, and Yue Zhao. 2023. Weakly supervised anomaly detection: A survey. *arXiv preprint arXiv:2302.04549* (2023).
- [26] Longlong Jing and Yingli Tian. 2020. Self-supervised visual feature learning with deep neural networks: A survey. *IEEE transactions on pattern analysis and machine intelligence* 43, 11 (2020), 4037–4058.
- [27] Mahmut Kaya and Hasan Şakir Bilge. 2019. Deep metric learning: A survey. *Symmetry* 11, 9 (2019), 1066.
- [28] Prannay Khosla, Piotr Teterwak, Chen Wang, Aaron Sarna, Yonglong Tian, Phillip Isola, Aaron Maschiot, Ce Liu, and Dilip Krishnan. 2020. Supervised contrastive learning. *Advances in neural information processing systems* 33 (2020), 18661–18673.
- [29] Hendrik Kuck and Nando De Freitas. 2012. Learning about individuals from group statistics. *arXiv preprint arXiv:1207.1393* (2012).
- [30] Laura Elena Cué La Rosa and Dário Augusto Borges Oliveira. 2022. Learning from label proportions with prototypical contrastive clustering. In *Proceedings of the AAAI Conference on Artificial Intelligence*, Vol. 36. 2153–2161.
- [31] Samuli Laine and Timo Aila. 2016. Temporal ensembling for semi-supervised learning. *arXiv preprint arXiv:1610.02242* (2016).
- [32] Jiabin Liu, Zhiquan Qi, Bo Wang, Yingjie Tian, and Yong Shi. 2022. SELF-LLP: Self-supervised learning from label proportions with self-ensemble. *Pattern Recognition* 129 (2022), 108767.
- [33] Jiabin Liu, Bo Wang, Hanyuan Hang, Huadong Wang, Zhiquan Qi, Yingjie Tian, and Yong Shi. 2022. LLP-GAN: A GAN-based algorithm for learning from label proportions. *IEEE transactions on neural networks and learning systems* (2022).
- [34] Jiabin Liu, Bo Wang, Xin Shen, Zhiquan Qi, and Yingjie Tian. 2021. Two-stage training for learning from label proportions. *arXiv preprint arXiv:2105.10635* (2021).
- [35] Takeru Miyato, Shin-ichi Maeda, Masanori Koyama, and Shin Ishii. 2018. Virtual adversarial training: a regularization method for supervised and semi-supervised learning. *IEEE transactions on pattern analysis and machine intelligence* 41, 8 (2018), 1979–1993.
- [36] David R Musicant, Janara M Christensen, and Jamie F Olson. 2007. Supervised learning by training on aggregate outputs. In *Seventh IEEE International Conference on Data Mining (ICDM 2007)*. IEEE, 252–261.
- [37] Jay Nandy, Rishi Saket, Prateek Jain, Jatin Chauhan, Balaraman Ravindran, and Aravindan Raghuvver. 2022. Domain-Agnostic Contrastive Representations for Learning from Label Proportions. In *Proceedings of the 31st ACM International Conference on Information & Knowledge Management*. 1542–1551.
- [38] Conor O'Brien, Arvind Thiagarajan, Sourav Das, Rafael Barreto, Chetan Verma, Tim Hsu, James Neufeld, and Jonathan J Hunt. 2022. Challenges and approaches to privacy preserving post-click conversion prediction. *arXiv preprint arXiv:2201.12666* (2022).
- [39] Augustus Odena. 2016. Semi-supervised learning with generative adversarial networks. *arXiv preprint arXiv:1606.01583* (2016).
- [40] Aaron van den Oord, Yazhe Li, and Oriol Vinyals. 2018. Representation learning with contrastive predictive coding. *arXiv preprint arXiv:1807.03748* (2018).
- [41] Guansong Pang, Longbing Cao, Ling Chen, and Huan Liu. 2018. Learning representations of ultrahigh-dimensional data for random distance-based outlier detection. In *Proceedings of the 24th ACM SIGKDD international conference on knowledge discovery & data mining*. 2041–2050.
- [42] Zhiquan Qi, Bo Wang, Fan Meng, and Lingfeng Niu. 2016. Learning with label proportions via NPSVM. *IEEE transactions on cybernetics* 47, 10 (2016), 3293–3305.
- [43] Novi Quadrianto, Alex J Smola, Tiberio S Caetano, and Quoc V Le. 2008. Estimating labels from label proportions. In *Proceedings of the 25th International Conference on Machine Learning*. 776–783.
- [44] Stefan Rueping. 2010. SVM classifier estimation from group probabilities. In *Proceedings of the 27th international conference on machine learning (ICML-10)*. 911–918.
- [45] Lukas Ruff, Robert A Vandermeulen, Nico Görmitz, Alexander Binder, Emmanuel Müller, Klaus-Robert Müller, and Marius Kloft. 2019. Deep semi-supervised anomaly detection. *arXiv preprint arXiv:1906.02694* (2019).
- [46] Ira Shavitt and Eran Segal. 2018. Regularization learning networks: deep learning for tabular datasets. *Advances in Neural Information Processing Systems* 31 (2018).
- [47] Gowthami Somepalli, Micah Goldblum, Avi Schwarzschild, C Bayan Bruss, and Tom Goldstein. 2021. Saint: Improved neural networks for tabular data via row attention and contrastive pre-training. *arXiv preprint arXiv:2106.01342* (2021).
- [48] Weiping Song, Chence Shi, Zhiping Xiao, Zhijian Duan, Yewen Xu, Ming Zhang, and Jian Tang. 2019. AutoInt: Automatic feature interaction learning via self-attentive neural networks. In *Proceedings of the 28th ACM international conference on information and knowledge management*. 1161–1170.
- [49] Marco Stolpe and Katharina Morik. 2011. Learning from label proportions by optimizing cluster model selection. In *Joint European Conference on Machine Learning and Knowledge Discovery in Databases*. Springer, 349–364.
- [50] Waqas Sultani, Chen Chen, and Mubarak Shah. 2018. Real-world anomaly detection in surveillance videos. In *Proceedings of the IEEE conference on computer vision and pattern recognition*. 6479–6488.
- [51] Tao Sun, Dan Sheldon, and Brendan O'Connor. 2017. A probabilistic approach for learning with label proportions applied to the us presidential election. In *2017 IEEE International Conference on Data Mining (ICDM)*. IEEE, 445–454.
- [52] Latanya Sweeney. 2002. k-anonymity: A model for protecting privacy. *International journal of uncertainty, fuzziness and knowledge-based systems* 10, 05 (2002), 557–570.

- [53] Bowen Tian, Qinliang Su, and Jian Yin. 2022. Anomaly detection by leveraging incomplete anomalous knowledge with anomaly-aware bidirectional gans. *arXiv preprint arXiv:2204.13335* (2022).
- [54] Yu Tian, Guansong Pang, Yuanhong Chen, Rajvinder Singh, Johan W Verjans, and Gustavo Carneiro. 2021. Weakly-supervised video anomaly detection with robust temporal feature magnitude learning. In *Proceedings of the IEEE/CVF international conference on computer vision*. 4975–4986.
- [55] Kuen-Han Tsai and Hsuan-Tien Lin. 2020. Learning from label proportions with consistency regularization. In *Asian Conference on Machine Learning*. PMLR, 513–528.
- [56] Yao-Hung Hubert Tsai, Tianqin Li, Weixin Liu, Peiyuan Liao, Ruslan Salakhutdinov, and Louis-Philippe Morency. 2022. Learning weakly-supervised contrastive representations. *arXiv preprint arXiv:2202.06670* (2022).
- [57] Hsiao-Yu Tung, Hsiao-Wei Tung, Ersin Yumer, and Katerina Fragkiadaki. 2017. Self-supervised learning of motion capture. *Advances in neural information processing systems* 30 (2017).
- [58] Talip Ucar, Ehsan Hajiramezanali, and Lindsay Edwards. 2021. Subtab: Subsetting features of tabular data for self-supervised representation learning. *Advances in Neural Information Processing Systems* 34 (2021), 18853–18865.
- [59] Ashish Vaswani, Noam Shazeer, Niki Parmar, Jakob Uszkoreit, Llion Jones, Aidan N Gomez, Łukasz Kaiser, and Illia Polosukhin. 2017. Attention is all you need. *Advances in neural information processing systems* 30 (2017).
- [60] Pascal Vincent, Hugo Larochelle, Yoshua Bengio, and Pierre-Antoine Manzagol. 2008. Extracting and composing robust features with denoising autoencoders. In *Proceedings of the 25th international conference on Machine learning*. 1096–1103.
- [61] Boyang Wan, Yuming Fang, Xue Xia, and Jiajie Mei. 2020. Weakly supervised video anomaly detection via center-guided discriminative learning. In *2020 IEEE international conference on multimedia and expo (ICME)*. IEEE, 1–6.
- [62] Bo Wang, Yingte Sun, and Qiang Tong. 2023. LLP-AAE: Learning from label proportions with adversarial autoencoder. *Neurocomputing* 537 (2023), 282–295.
- [63] Junyuan Xie, Ross Girshick, and Ali Farhadi. 2016. Unsupervised deep embedding for clustering analysis. In *International conference on machine learning*. PMLR, 478–487.
- [64] Tiansheng Yao, Xinyang Yi, Derek Zhiyuan Cheng, Felix Yu, Ting Chen, Aditya Menon, Lichan Hong, Ed H Chi, Steve Tjoa, Jieqi Kang, et al. 2021. Self-supervised learning for large-scale item recommendations. In *Proceedings of the 30th ACM International Conference on Information & Knowledge Management*. 4321–4330.
- [65] Jinsung Yoon, Yao Zhang, James Jordon, and Mihaela van der Schaar. 2020. Vime: Extending the success of self-and semi-supervised learning to tabular domain. *Advances in Neural Information Processing Systems* 33 (2020), 11033–11043.
- [66] Felix X Yu, Krzysztof Choromanski, Sanjiv Kumar, Tony Jebara, and Shih-Fu Chang. 2014. On learning from label proportions. *arXiv preprint arXiv:1402.5902* (2014).
- [67] Shuai Yuan, Jun Wang, and Xiaoxue Zhao. 2013. Real-time bidding for online advertising: measurement and analysis. In *Proceedings of the seventh international workshop on data mining for online advertising*. 1–8.
- [68] Sangdoo Yun, Dongyoon Han, Seong Joon Oh, Sanghyuk Chun, Junsuk Choe, and Youngjoon Yoo. 2019. Cutmix: Regularization strategy to train strong classifiers with localizable features. In *Proceedings of the IEEE/CVF international conference on computer vision*. 6023–6032.
- [69] Xiaohua Zhai, Avital Oliver, Alexander Kolesnikov, and Lucas Beyer. 2019. S4l: Self-supervised semi-supervised learning. In *Proceedings of the IEEE/CVF international conference on computer vision*. 1476–1485.
- [70] Hongyi Zhang, Moustapha Cisse, Yann N Dauphin, and David Lopez-Paz. 2017. mixup: Beyond empirical risk minimization. *arXiv preprint arXiv:1710.09412* (2017).
- [71] Jianxin Zhang, Yutong Wang, and Clay Scott. 2022. Learning from label proportions by learning with label noise. *Advances in Neural Information Processing Systems* 35 (2022), 26933–26942.
- [72] Yue Zhao, Guoqing Zheng, Subhabrata Mukherjee, Robert McCann, and Ahmed Awadallah. 2023. Admoe: Anomaly detection with mixture-of-experts from noisy labels. In *Proceedings of the AAAI Conference on Artificial Intelligence*, Vol. 37. 4937–4945.
- [73] Jia-Xing Zhong, Nannan Li, Weijie Kong, Shan Liu, Thomas H Li, and Ge Li. 2019. Graph convolutional label noise cleaner: Train a plug-and-play action classifier for anomaly detection. In *Proceedings of the IEEE/CVF conference on computer vision and pattern recognition*. 1237–1246.
- [74] Zhi-Hua Zhou. 2018. A brief introduction to weakly supervised learning. *National science review* 5, 1 (2018), 44–53.

## A METHODOLOGY

### A.1 Pseudo Code.

We present the pseudo-code for our proposed TabLLP-BDC methodology, encapsulated in Algo. 1. The algorithm details the complete process of our approach, divided into two distinct phases: Bag Contrastive Pretraining and Difference Contrastive Fine-tuning.

During the Bag Contrastive Pretraining phase, the algorithm iteratively processes pairs of bags from the LLP dataset  $D$ . For each pair, it computes embeddings for all instances using the encoder  $f_\theta$  and projects these embeddings via  $g_\delta$ . It then calculates the aggregated bag representations using the weighted sum aggregation mechanism discussed in Sec. 3.3. The pretraining loss comprises the Bag Contrastive loss  $\mathcal{L}_{Bag}$ , the Self-contrastive loss, and the Denoising Reconstruction loss.

In the Difference Contrastive Fine-tuning phase, the model further refines its understanding of the data. For each pair of bags, embeddings are again computed for all instances. Pseudo-positive and pseudo-negative pairs are generated based on label proportions, facilitating the creation of instance-level supervision signals. The fine-tuning loss is a weighted combination of the Difference Contrastive loss  $\mathcal{L}_{Diff}$  and the classical LLP loss  $\mathcal{L}_{LLP}$ . The exponential ramp-up and ramp-down weights  $\lambda(t)$  and  $\gamma(t)$  dynamically adjust the emphasis between two losses across fine-tuning epochs.

---

#### Algorithm 1: TabLLP-BDC Methodology

---

**Input:** LLP Dataset  $D = \{(B_k, \hat{p}_k)\}_{k=1}^K$   
**Output:** Optimized model parameters  $\theta^*, \omega^*$   
 /\* Phase 1: Bag Contrastive Pretraining \*/

```

1 foreach pretraining epoch  $e$  do
2   foreach pair of bags  $(B_{k1}, B_{k2})$  from  $D$  do
3     Compute embeddings  $z_i = f_\theta(x_i)$  for all  $x_i \in B_{k1} \cup B_{k2}$ 
4     Compute projection  $j_i = g_\delta(z_i)$ 
5     Compute bag representation  $b_{k1}, b_{k2}$  using aggregation mechanism
6     Update  $\theta, \delta$  by minimizing
        $\alpha \mathcal{L}_{Bag}(\{b_{k1}, b_{k2}\}, \{\hat{p}_{k1}, \hat{p}_{k2}\}) + \beta \mathcal{L}_{Self}(J)$ 
7   end
8 end
  /* Phase 2: Difference Contrastive Fine-tuning */
9 foreach fine-tuning epoch  $t$  do
10   foreach pair of bags  $(B_{k1}, B_{k2})$  from  $D$  do
11     Compute embeddings  $z_i = f_\theta(x_i)$  for all  $x_i \in B_{k1} \cup B_{k2}$ 
12     Generate pseudo-positive and pseudo-negative pairs  $P, Q$ 
13     Compute prediction logic  $\hat{y}_i = h_\omega(z_i)$  and then proportion  $\hat{p}_k$ 
14     Update  $\theta, \omega$  by minimizing
        $\lambda(t) \mathcal{L}_{Diff}(Z, P) + \gamma(t) \mathcal{L}_{LLP}(\{\hat{p}_{k1}, \hat{p}_{k2}\}, \{\hat{p}_{k1}, \hat{p}_{k2}\})$ 
15   end
16 end
17 return  $\theta^*, \omega^*$ 

```

---

### A.2 Model Architecture.

Our primary objective is to learn a robust, discriminative, and class-aware representation of tabular data in the LLP landscape. To

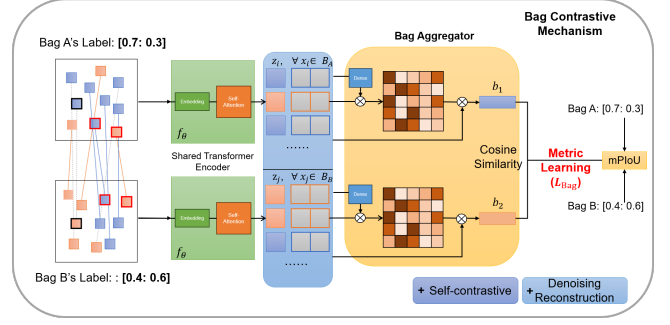


**Figure 4: Overview of TabLLP-BDC's Bag Contrastive Mechanism.**

address the challenges inherent in tabular-based LLP, we introduce a novel architecture that leverages the strengths of transformer models [59] while introducing new components tailored to our LLP paradigm. In our proposed architecture, we utilize a SOTA transformer model called SAINT [47] in the deep tabular learning domain as the backbone encoder. Building upon SAINT's success in supervised and semi-supervised settings, this design prioritizes both robustness and performance, emphasizing the extraction of high-quality tabular representations. The encoder processes input embeddings using multi-head self-attention and intersample attention, mechanisms that highlight the importance of individual features and capture intricate relationships within or between the data. Mathematically, the SAINT model can be described by its forwarding equations [47]:

$$\begin{aligned}
 z_i^{(1)} &= \text{LN}(\text{MSA}(E(x_i))) + E(x_i) \\
 z_i^{(2)} &= \text{LN}(\text{FF}_1(z_i^{(1)})) + z_i^{(1)} \\
 z_i^{(3)} &= \text{LN}(\text{MISA}(\{z_i^{(2)}\}_{i=1}^b)) + z_i^{(2)} \\
 z_i &= \text{LN}(\text{FF}_2(z_i^{(3)})) + z_i^{(3)}
 \end{aligned}$$

where  $z_i$  is SAINT's contextual representation output corresponding to data point  $x_i$ ,  $\text{MSA}(\cdot)$  represents multi-head self-attention,  $\text{MISA}(\cdot)$  represents multi-head intersample attention,  $\text{FF}$  denotes feed-forward layers,  $\text{LN}$  stands for layer normalization, and  $b$  is the batch size. The embedding layer,  $E$ , is a unique aspect of SAINT, using different embedding functions for different features and missing value embedding for imputation. Let  $x_i = [[\text{CLS}], f_i^{\{1\}}, \dots, f_i^{\{n\}}]$  be a single data-point with categorical or continuous features, the model exclusively channels the CLS token into an MLP-based prediction head to produce the logic for classification.

To further refine our data representations for LLP during pretraining, we have designed a Bag Aggregator, as illustrated in Fig. 4. This component crafts a bag representation by aggregating instance representations, weighted based on intersample similarity. Its primary function is to emphasize instance-wise similarity in determining the contribution of each instance. Moreover, our model is equipped with a Pseudo-pairs Generator for the Difference Contrastive learning task, as illustrated in Fig. 1. This component leverages linear programming of the linear sum assignment problem to generate pseudo-positive and negative pairs, augmenting the LLP

training process with *class-aware* instance-level supervision signals. In summary, our architecture amalgamates the strengths of the SAINT encoder in learning tabular representation with novel components tailored for our two-stage LLP training strategy, ensuring outstanding performance for our task.

### A.3 Pretraining Pool.

We incorporate two additional losses from SAINT [47] into our pre-training pool. The first, a Self-contrastive loss, minimizes the distance between latent representations of two different views of the same data point ( $z_i$  and  $z'_i$ ), while maximizing the distance between distinct data points ( $z_i$  and  $z_j$ ,  $i \neq j$ ). This employs the InfoNCE loss [21, 40], a metric from metric-learning literature. The second loss is derived from a denoising task aimed at reconstructing the original data sample from its noisy view [47]. Given a noisy representation  $z'_i$ , the goal is to generate a reconstruction  $x''_i$  that minimizes the discrepancy between the original data and its reconstruction. The combined pre-training loss  $\mathcal{L}_{Self}$  is:

$$\mathcal{L}_{Self}(Z) = \mathcal{L}_{Self-contrastive}(Z) + \mathcal{L}_{Reconstruct}(Z)$$

$$\mathcal{L}_{Self-contrastive}(Z) = - \sum_{i=1}^m \log \frac{\exp(z_i \cdot z'_i / \tau)}{\sum_{k=1}^m \exp(z_i \cdot z'_k / \tau)}$$

$$\mathcal{L}_{Reconstruct}(Z) = \kappa \sum_{i=1}^m \sum_{j=1}^n [\mathcal{L}_j(\text{MLP}_j(z'_i), x_i)]$$

Here,  $e_i = E(x_i)$  is the original embedding,  $f_\theta$  is the encoder,  $z_i = f_\theta(e_i)$ ,  $z'_i = f_\theta(e'_i)$ ,  $z_i = g_1(z_i)$ ,  $z'_i = g_2(z'_i)$ ,  $\kappa$  is a hyper-parameter, and  $\tau$  is temperature parameter.  $\mathcal{L}$  is cross-entropy loss or mean squared error depending on the  $j$ th feature being categorical or continuous. The projectors include  $n$  single layer MLP with a ReLU non-linearity.

Following SAINT [47], we adopt the combination of MixUp and CutMix as the baseline augmentations to form a challenging yet effective Self-supervision task. Given a data point  $x_i$ , we compute its original embedding  $e_i = E(x_i)$ . The augmented representation, denoted as  $e'_i$ , is generated through a combination of MixUp [70] and CutMix [68] techniques as follows:

$$\begin{aligned} x'_i &= x_i \odot n_m + x_a \odot (1 - n_m) \\ e'_i &= n_u * E(x'_i) + (1 - n_u) * E(x'_b) \end{aligned}$$

where  $x_a$  and  $x_b$  are randomly selected samples from the same batch,  $x'_b$  represents the CutMix variant of  $x_b$ ,  $n_m$  is a binary mask vector drawn from a Bernoulli distribution with probability  $p_{\text{cutmix}}$ , and  $n_u$  is the MixUp parameter influencing the blend ratio. This effective augmentation strategy stands for the major comparison baseline of our augmentation-free separated representation approach.

## B EXPERIMENTAL SETTINGS

### B.1 Datasets and Preprocess.

In total, our study utilizes eight datasets: seven public tabular datasets (five medium sizes, two large sizes) sourced from OpenML<sup>3</sup> and a private dataset from the gaming industry. The statistics of the datasets are shown in Tab. 8. We allocate the datasets into an 80%/10%/10% split for training, testing, and validation, respectively.

<sup>3</sup><https://www.openml.org/>

**Table 8: Dataset Statistics.**

Dataset	ID	Size	Numeric	Categorical	Classes
AD	1590	48842	6	9	2
BA	1461	45211	7	10	2
CA	44090	20634	8	1	2
CR	44089	16714	10	1	2
EL	44156	38474	7	2	2
RO	44161	111762	29	4	2
Movielens-1M	-	739012	3	4	2
Private	-	>300000	69	11	2/3

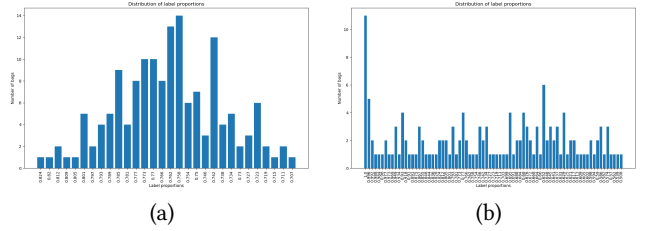


**Figure 5: The bag label proportion distribution after adopting (a) random bagging, and (b) ordered bagging on AD dataset.**

**Table 9: Analysis of Bagging Strategies across Datasets.**

Model	Strat.	AUC (%)					
		AD	BA	CA	CR	EL	RO
DLLP	Rand.	<b>85.07</b>	80.43	78.34	63.08	72.53	65.96
DLLP	<b>Ord.</b>	87.49	<b>78.27</b>	<b>79.82</b>	<b>75.02</b>	<b>74.90</b>	<b>78.99</b>
TabLLP-BDC	Rand.	85.92	70.68	82.16	71.90	74.84	67.28
TabLLP-BDC	<b>Ord.</b>	<b>87.81</b>	<b>84.95</b>	<b>84.85</b>	<b>79.29</b>	<b>77.53</b>	<b>79.67</b>

In addition to the fact that the labels of real datasets are inherently in the form of label proportion, we use two different black-box bagging strategies for public datasets to simulate practical application scenarios, as discussed in the following Sec. B.2 Bagging Process.

Adhering to the preprocessing standards set by [3, 20, 47], we employ one-hot encoding for categorical features and Z-normalize numerical features. For public datasets, rather than conventional imputation methods like mean imputation, we leverage the missing value embedding technique from SAINT [47]. For the private dataset, numerical missing values are imputed with zero due to domain specificity, while missing value embedding is reserved for categorical features.

### B.2 Bagging Process

We explore two black-box bagging strategies for the LLP simulation of public datasets: random bagging and ordered bagging. This is because in reality, the label proportion within each bag cannot be validated or explored before bagging and querying the data for response, and no adjustments on bagging can be made post-querying for differential check policy [12]. Random bagging disregards feature correlations and aggregates instances arbitrarily. In contrast, ordered bagging sequences instances based on raw features, grouping similar instances—a rapid variant of clustering for large datasets. Both methods operate under the assumption of no prior domain knowledge. This mirrors the constraints of aggregated reporting

**Table 10: Analysis of Transformer Encoder Configurations.**

Architecture	AUC (%)					
	AD	BA	CA	CR	EL	RO
colrow-1	85.88	<b>82.76</b>	<b>80.76</b>	69.84	73.44	74.2
<b>col-6</b>	<b>87.49</b>	78.27	79.82	<b>75.02</b>	<b>74.90</b>	<b>78.99</b>

[12] and K-anonymity [52], preventing illegal instance-level data extraction from aggregated datasets. As illustrated in the accompanying Fig. 5 and Tab. 9, ordered bagging consistently surpasses random bagging across various models, attributed to its diverse label proportions. Consequently, our study exclusively employs the ordered bagging strategy.

### B.3 Model Implementation and Training Setting

As detailed in Sec.A.2, TabLLP-BDC’s architecture encompasses an encoder, a CLS token MLP, dual Self-contrastive pretraining projectors, a reconstruction decoder, a bag aggregator, a Bag Contrastive pretraining projector, and a pseudo-pairs generator. Unless otherwise stated, the SAINT model [47] serves as the encoder for all tabular model variants. Despite SAINT’s intersample version’s superior performance in supervised and semi-supervised tabular data settings, our findings in Tab. 10 indicate no performance enhancement from combining intersample attention and self-attention in LLP. Thus, we utilize SAINT’s 6-layer multi-head self-attention variant with recommended hyperparameters<sup>4</sup>. The CLS token MLP and projectors are 3-layer MLP with ReLU activation, while the reconstruction decoder takes separated MLP for each feature token. We implement the bag aggregator as the weighted sum of instance representation based on intersample cosine similarity, as introduced in Sec. 3.3. The pseudo-pairs generator is achieved by the publicly available implementation<sup>5</sup> of the modified Jonker-Volgenant algorithm [9]. But we also studied other possible implementations, summarized in Tab. 11, in the following ablation studies.

Our training bifurcates into pretraining and finetuning phases. The pretraining phase adopts a multi-task approach, integrating Denoising Reconstruction [47, 60], Self-contrastive [3, 8, 40], and Bag Contrastive methods. Feature Mixup [47, 65, 68, 70] serves as the default pretraining augmentation for Self-contrastive. The finetuning phase’s objective melds a ramping-down LLP Loss [1] with a ramping-up Difference Contrastive Loss. We use 50 epochs for the pretraining phase and 300 epochs for the finetuning phase, with an early stopping of 20 epochs on the validation AUC score or mPIoU score based on the real-world LLP scenario. The other optimal training hyperparameter is tuned using Optuna<sup>6</sup> with 50 trials for each dataset and model. We repeat 10 trials for each experiment using different train/validation/test splits. All experiments can be reproduced using a single GeForce RTX 2080 GPU.

<sup>4</sup><https://github.com/somepago/saint>

<sup>5</sup>[https://docs.scipy.org/doc/scipy/reference/generated/scipy.optimize.linear\\_sum\\_assignment.html](https://docs.scipy.org/doc/scipy/reference/generated/scipy.optimize.linear_sum_assignment.html)

<sup>6</sup><https://optuna.org/>

### B.4 Baselines

Given the nascent exploration of LLP in tabular data, we also adapt several leading LLP image data baselines and introduce intuitive baselines for pure tabular scenarios. The details of selected baselines are listed below:

- DLLP [1]: The classical and fundamental work that proposed the LLP Loss for LLP training for image data. The design also utilizes co-trained images, text, and various label-invariant image distortions, such as rotation and flipping. We only keep the LLP Loss because our task scenario does not satisfy multimodal data and label-invariant augmentation. We replace the Xception (for image input) and MLP (for text input) backbones with a single SOTA supervised deep tabular learning model [47] we adopted in the study for a fair comparison. DLLP stands as a primary comparison model in our ablation study, highlighting the enhanced performance offered by the Difference Contrastive objective.
- LLP-GAN [33]: A classical work that leverages the power of SGAN [39] to LLP. The architecture consists of a generator and a discriminator (K+1-way classifier). It combines the traditional GAN loss with LLP Loss [1] to encourage the predicted label proportions to match the true label proportions. The work is proposed for image data. To tackle the challenge of generating categorical features and realistic tabular samples, we adopt the design of cWGAN [16] as the backbone for the generator and discriminator while the training objective and procedure remain consistent with LLP-GAN.
- LLP-VAT [55]: A notable work that applies consistency regularization upon the LLP Loss [1] with the help of Virtual Adversarial Training [35]. The model will learn to be robust to adversarial perturbations, which can improve its generalization ability. The work is proposed for image data but can be directly transferred to tabular data. The backbone encoder is upgraded to the same model [47] we used in our model architecture.
- SelfCLR-LLP [37]: To the best of our knowledge, it is the only work that tackles the LLP problem in tabular data. The model combines the Self-contrastive loss with the LLP Loss [1] to promote controlled diversity in the representations. The original backbone was AutoInt [48], and we replaced it with a more recent model [47], as in our general model setting, for fairness. SelfCLR-LLP stands as a primary comparison model in our ablation study, highlighting the enhanced performance offered by the Difference Contrastive objective.
- TabLLP-DEC: DEC [63] is a typical deep clustering model in an unsupervised data setting. The model continuously updates the embeddings of the centroids during the training process by fitting the student’s t-distribution. An intuitive modification to transfer it to the LLP setting as a baseline is to add the LLP Loss [1] to its clustering loss. The encoder is the same as the other models [47] in the experiment.
- TabLLP-PSE: Pseudo-labeling is another typical approach [6, 34] to further finetune bag-level training with instance-level pseudo-labels. We implement constrained KMeans to generate pseudo-labels that exactly match the bag label proportion and perform supervised learning with respect to pseudo-labels in the second stage after initial training with the LLP Loss [1]. The encoder is the same as the other models [47] in the experiment.

**Table 11: Summary of Model Design Components.**

Component	Options
<b>Augmentation</b>	Separated Representation (Sec. A.2), Feature Mixup (Sec. A.3), Full Representation
<b>Pretraining Task</b>	Bag Contrastive (Sec. 3.3), Self-contrastive (Sec. A.3), Denoising Reconstruction (Sec. A.3)
<b>Bag Aggregator</b>	Cosine similarity (Sec. 3.3), Intersample attention mechanism (Sec. A.2), Cosine similarity + projection, Intersample attention mechanism + projection
<b>Difference Contrastive Objective</b>	Supervised InfoNCE (Sec. 3.2), Cosine Embedding (Sec. D.2), Self-contrastive
<b>Pseudo-pairs Generator</b>	Linear Sum Assignment (Sec. 3.2), Greedy Nearest Neighbor Assignment (Sec. D.2)
<b>Bag-level Validation Metric</b>	L1, mPIoU (Sec. 4.1.3)

**Table 12: Coarse-grained Experimental Results.**

	AUC (%)						Accuracy (%)	
	AD	BA	CA	CR	EL	RO	Private A	Private B
Fine-grained	87.81 $\pm$ 0.18	84.95 $\pm$ 1.88	84.85 $\pm$ 0.93	79.29 $\pm$ 0.39	77.53 $\pm$ 1.48	79.67 $\pm$ 0.25	51.39 $\pm$ 0.16	74.03 $\pm$ 1.54
DLLP	87.22 $\pm$ 0.65	75.94 $\pm$ 1.86	76.87 $\pm$ 1.28	74.22 $\pm$ 0.45	71.37 $\pm$ 1.58	78.89 $\pm$ 0.55	46.22 $\pm$ 0.54	63.43 $\pm$ 1.56
LLP-GAN	82.45 $\pm$ 0.90	70.44 $\pm$ 0.60	80.08 $\pm$ 1.75	64.44 $\pm$ 1.78	53.16 $\pm$ 1.30	70.72 $\pm$ 0.79	44.67 $\pm$ 1.06	62.76 $\pm$ 1.48
LLP-VAT	83.03 $\pm$ 1.83	77.69 $\pm$ 2.15	77.25 $\pm$ 2.32	72.09 $\pm$ 1.18	72.03 $\pm$ 2.05	77.76 $\pm$ 0.80	48.49 $\pm$ 1.15	62.23 $\pm$ 5.48
SelfCLR-LLP	86.14 $\pm$ 0.77	72.79 $\pm$ 4.06	79.28 $\pm$ 0.82	74.59 $\pm$ 0.60	69.59 $\pm$ 4.00	78.53 $\pm$ 0.14	48.88 $\pm$ 0.50	63.26 $\pm$ 4.16
TabLLP-DEC	59.32 $\pm$ 8.78	55.03 $\pm$ 3.37	79.64 $\pm$ 1.17	73.79 $\pm$ 1.18	68.16 $\pm$ 4.70	62.59 $\pm$ 1.70	45.54 $\pm$ 1.64	52.21 $\pm$ 1.96
TabLLP-PSE	86.15 $\pm$ 1.01	76.47 $\pm$ 2.48	75.89 $\pm$ 1.97	75.35 $\pm$ 1.70	64.93 $\pm$ 8.55	78.14 $\pm$ 0.13	43.49 $\pm$ 2.04	57.46 $\pm$ 3.38
TabLLP-SELF	85.00 $\pm$ 0.54	78.22 $\pm$ 1.14	79.19 $\pm$ 1.93	75.67 $\pm$ 0.65	70.16 $\pm$ 3.51	78.86 $\pm$ 0.31	49.28 $\pm$ 0.86	56.12 $\pm$ 1.72
<b>TabLLP-BDC</b>	<b>87.41 <math>\pm</math> 0.35</b>	<b>83.81 <math>\pm</math> 1.67</b>	<b>80.23 <math>\pm</math> 1.37</b>	<b>78.49 <math>\pm</math> 0.25</b>	<b>73.52 <math>\pm</math> 0.90</b>	<b>79.34 <math>\pm</math> 0.32</b>	<b>50.24 <math>\pm</math> 1.21</b>	<b>64.99 <math>\pm</math> 1.29</b>

**Table 13: Relationship between mPIoU and AUC Metrics.**

Model	Metric	Dataset				
		AD	BA	CA	CR	EL
Supervised	mPIoU	87.76	<b>90.23</b>	<b>97.90</b>	87.05	<b>95.14</b>
Supervised	AUC	<b>91.37</b>	<b>94.01</b>	<b>95.87</b>	<b>82.36</b>	<b>90.73</b>
DLLP	mPIoU	94.55	78.59	96.01	<b>93.17</b>	91.96
DLLP	AUC	87.22	75.94	76.87	74.22	71.37
TabLLP-BDC	mPIoU	<b>94.96</b>	78.78	95.72	93.09	94.92
TabLLP-BDC	AUC	87.41	83.81	80.23	78.49	73.52

- TabLLP-SELF: This variant draws inspiration from SelfCLR-LLP [37]. However, it diverges by employing traditional Self-contrastive learning [3, 47] with feature mixup augmentation [47, 65, 68, 70] as its auxiliary loss. The encoder configuration aligns with that of other baselines [47]. TabLLP-Self stands as a primary comparison model in our ablation study, highlighting the enhanced performance offered by the Difference Contrastive objective.

## C EXPERIMENTAL RESULTS

We present the remaining experimental results as follow:

- The hidden instance-level test performance of the coarse-grained validation scenario is reported in Tab. 12. Our TabLLP-BDC achieved SOTA performance in the practical scenario devoid of fine-grained validation.
- Relationship between mPIoU and AUC metrics can be observed in Tab. 13. The imperfect correlation between the best instance-level predictions and label proportions validates our hypothesis

that solely relying on bag-level supervision is insufficient for accurate instance-level prediction in tabular data.

## D ABLATION STUDY

We present a comprehensive ablation study to assess the individual and combined effectiveness of the components, as summarized in Tab. 11, within our TabLLP-BDC model, including the studies of pretraining tasks, augmentation technique, bag aggregator, downstream contrastive objectives, pseudo-pairs generator, and mPIoU evaluation metric. For consistency, all experiments are conducted with a fixed bag size of 256 across five medium-sized public datasets, each with accessible fine-grained validation. Hyperparameters are meticulously tuned for each study.

### D.1 Ablation Study of Downstream Contrastive Objectives

In this section, we evaluate the performance of different finetuning objectives, ensuring the pretraining task remains constant. Specifically, our focus is on the following contrastive-based finetuning objectives: LLP loss [1], the loss proposed in SelfCLR-LLP [37], LLP loss + Self-contrastive [8] (similar to SelfCLR-LLP [37] but using Feature Mixup augmentation [47, 65, 68, 70]), and LLP loss + Difference Contrastive. When evaluating each finetuning objective, we consider two distinct pretraining scenarios: using the best pretraining tasks combination identified for each finetuning objective from our previous experiments in Tab. 7, and a scenario without any pretraining. As shown in Tab. 14, Our Difference Contrastive model shows superior performance compared to all the other contrastive-based objectives in most scenarios and datasets. To highlight, when



**Table 14: Ablation Study of Downstream Contrastive Objectives.**

Pretrain	Model	AUC (%)				
		AD	BA	CA	CR	EL
No	DLLP	<b>87.64</b>	77.18	78.75	75.07	74.33
No	SelfCLR	87.44	79.73	81.34	75.43	74.44
No	SELF	86.66	79.38	<b>82.55</b>	77.04	74.87
No	BDC	87.03	<b>81.77</b>	80.64	<b>79.10</b>	<b>75.43</b>
Optimal	DLLP	87.76	84.36	84.40	75.60	75.64
Optimal	SelfCLR	87.67	83.50	84.78	76.13	75.40
Optimal	SELF	86.99	83.16	84.19	77.69	75.44
Optimal	BDC	<b>87.81</b>	<b>84.95</b>	<b>84.85</b>	<b>79.29</b>	<b>77.53</b>

**Table 15: Ablation Study of Pseudo-pairs Generator.**

Assignment	AUC (%)				
	AD	BA	CA	CR	EL
Greedy	87.57	84.46	<b>85.31</b>	<b>79.66</b>	76.01
<b>Linear</b>	<b>87.81</b>	<b>84.95</b>	84.85	79.29	<b>77.53</b>

**Table 16: Ablation Study of Difference Contrastive Loss.**

Loss Function	AUC (%)				
	AD	BA	CA	CR	EL
CosineEmbedding	<b>87.81</b>	83.40	<b>84.85</b>	75.84	75.41
<b>SupInfoNCE</b>	87.33	<b>84.95</b>	84.43	<b>79.29</b>	<b>77.53</b>

combined with the best pretraining task for each objective, the best performance is always achieved by our Difference Contrastive objectives.

## D.2 Ablation Study of Downstream Components

To further refine the generation of pseudo-positive pairs, we introduce two methodologies: Linear Sum Assignment [9] and Greedy Nearest Neighbor Assignment. Additionally, we explore two learning objectives: the Supervised InfoNCE-based Contrastive loss and the Cosine Embedding loss<sup>7</sup>. The Greedy Nearest Neighbor Assignment will iterate through the similarity matrix to greedily extract the highest similarity 1-to-1 pairs to generate pseudo-positive pairs. The Cosine Embedding loss will treat the remaining pairs as pseudo-negative pairs and encourage the two sample representations to be similar or dissimilar based on both positive and negative pairs. Tab. 15 and Tab. 16 show that the Linear Sum Assignment and the Supervised InfoNCE-based Contrastive loss have empirically better performance. Please note that while the performance gap between the two generators is small, the Linear Sum Assignment has a significant efficiency advantage over the Greedy Nearest Neighbor Assignment in the implementation, which is crucial for operations that run every mini-batch. Therefore, we recommend using the Linear Sum Assignment for a practical balance between effectiveness and efficiency.

<sup>7</sup><https://pytorch.org/docs/stable/generated/torch.nn.CosineEmbeddingLoss.html>

**Table 17: Ablation Study of Augmentation.**

Model	Augment.	AUC (%)				
		AD	BA	CA	CR	EL
DLLP	FM	87.46	81.43	<b>83.53</b>	75.52	<b>75.31</b>
DLLP	SR	<b>87.55</b>	<b>84.36</b>	82.30	<b>75.58</b>	75.24
BDC	FM	<b>87.79</b>	82.18	<b>84.85</b>	<b>79.29</b>	<b>76.24</b>
BDC	SR	<b>87.79</b>	<b>84.95</b>	81.85	79.18	<b>76.24</b>

## D.3 Ablation Study of Pretraining Tasks

In this section, we evaluate the performance of various pretraining tasks, ensuring the finetuning objective remains constant throughout. Following the standard pretraining methodology outlined in [47] and the Sec. A.3, we consistently employ the denoising reconstruction task. Our primary focus is on the contrastive task, where we juxtapose the baseline Self-contrastive [3, 47] approach with our proposed Bag Contrastive method. The results from this comparison in Tab. 7 shed light on the impact of different pretraining contrastive tasks under three distinct finetuning objectives: the LLP loss [1], the loss proposed in SelfCLR-LLP [37], LLP loss + Self-contrastive [8] (similar to SelfCLR-LLP [37] but using Feature Mixup augmentation [47, 65, 68, 70]), and LLP loss + Difference Contrastive. Notably:

- The inclusion of a pretraining phase consistently enhances performance, emphasizing its critical role in label proportion learning from tabular data.
- Our Bag Contrastive pretraining emerges as a pivotal component, effectively bridging the gap between instance-level pretraining and bag-level finetuning.
- The introduction of the Difference Contrastive sometimes diminishes the distinct advantages of our Bag Contrastive, suggesting potential overlaps or redundancies between the two.

This study underscores a key insight: our Bag Contrastive and Difference Contrastive, which emphasize bag-level pretraining and instance-level supervision respectively, are designed to complement and enhance the instance-level pretraining offered by the Self-contrastive method [3, 47] and the bag-level supervision provided by the LLP loss [1] respectively. Their major role is to bolster the consistency between learning and prediction. However, since they both narrow the gap of LLP difficulty toward each other, they do not seem to significantly amplify each other's benefits together.

## D.4 Ablation Study of Pretraining Components

Furthermore, our study delves into two essential components of the pretraining task: data augmentation and bag aggregation.

Given the inherent challenges of generating label-invariant data augmentation for tabular data, we introduce an augmentation-free approach that uses bag comparison instead. However, by leveraging the capabilities of the CLS token in the Tabular Transformer [19, 47], we also propose to adopt representation separation to extract two label-invariant views of samples directly. This approach mirrors the idea of subsetting raw features in SubTab [58] but is executed in the representation space using the CLS token and basic representation space. Our experiments in Tab. 17, comparing this separated representation (SR) technique with the classical feature mixup (FM)

**Table 18: Ablation Study of Bag Aggregation Techniques.**

Model	Augment.	AUC (%)				
		AD	BA	CA	CR	EL
BDC	WS	87.74	<b>84.91</b>	83.55	<b>79.16</b>	<b>77.53</b>
BDC	IA	<b>87.81</b>	84.42	83.75	79.00	77.22
BDC	WS-Proj	87.64	84.11	<b>83.94</b>	78.72	76.37
BDC	IA-Proj	87.65	83.85	80.93	79.13	76.45

**Table 19: Ablation Study of Bag-Level Metrics in Early Stopped LLP Models.**

Model	Metrics	AUC (%)				
		AD	BA	CA	CR	EL
van. DLLP	L1	<b>87.22</b>	<b>75.94</b>	74.42	73.50	69.68
van. DLLP	<b>mPIoU</b>	86.62	74.20	<b>76.87</b>	<b>74.22</b>	<b>71.37</b>
DLLP	L1	<b>87.32</b>	77.84	78.45	<b>74.69</b>	70.00
DLLP	<b>mPIoU</b>	87.30	<b>80.74</b>	<b>78.85</b>	74.03	<b>72.29</b>
SELF	L1	84.38	<b>80.01</b>	<b>80.72</b>	75.57	72.95
SELF	<b>mPIoU</b>	<b>85.13</b>	79.96	80.46	<b>76.43</b>	<b>73.29</b>
BDC	L1	86.80	83.14	78.64	78.25	70.35
BDC	<b>mPIoU</b>	<b>87.41</b>	<b>83.81</b>	<b>80.23</b>	<b>78.49</b>	<b>73.52</b>

method [47, 65, 68, 70], reveal varied performance across datasets. However, our separated representation offers a slight efficiency advantage as it avoids direct sample manipulation.

In our exploration of aggregation techniques, we compare the performance of a similarity-driven weighted sum aggregator (WS)

with an intersample attention-based aggregator (IA). The former calculates attention scores based on the cosine similarity between samples from the same bag, contributing to the overall bag representation. In contrast, the latter, inspired by the design of multi-head row attention in SAINT [47] and Sec. A.2, aggregates intersample representations into a singular bag representation vector using mean reduction. Our experiments shown in Tab. 18 indicate that the similarity-driven weighted sum aggregator, when used without projection, generally delivers superior performance.

## D.5 Evaluation of Bag-Level Metrics in Early Stopped LLP Models

We investigate the performance of LLP models that are early stopped using bag-level evaluation metrics. Specifically, we employ the L1 metric [55] and our mPIoU metric (Sec. 4.1.3). The context for this examination parallels the scenarios outlined in the Downstream Contrastive Objectives ablation study: using the best pretraining tasks combination except for the vanilla DLLP. Tab. 19 reveals that our mPIoU metric offers more counterpoint advantage over the L1. However, it is important to note that despite numerous experiments, some degree of fluctuation persists in the outcomes. Since this particular aspect is not the central focus of our study, we have incorporated both metrics in our prior Performance Evaluation of Coarse-grained Validation, selecting the highest results for presentation in Tab. 12. For future research, we advocate the consideration of both these metrics to ensure a comprehensive evaluation.

Received 20 February 2023; revised 12 March 2023; accepted 5 June 2023